A FULLY DISCRETE FINITE ELEMENT METHOD FOR A CONSTRAINED TRANSPORT MODEL OF THE INCOMPRESSIBLE MHD EQUATIONS

Xiaodi Zhang[1,2,3], Haiyan Su[4,*] AND Xianzhu Li[4]

Abstract. In this paper, we propose and analyze a fully discrete finite element method for a constrained transport (CT) model of the incompressible magnetohydrodynamic (MHD) equations. The spatial discretization is based on mixed finite elements, where the hydrodynamic unknowns are approximated by stable finite element pairs, the magnetic field and magnetic vector potential are discretized by $H(\mathbf{curl})$-conforming edge element. The time marching is combining a backward Euler scheme and some subtle implicit-explicit treatments for nonlinear and coupling terms. With these treatments, the fully discrete scheme is linear in the implementation and the computation of the magnetic vector potential is decoupled from the whole coupled system. The most attractive feature of this scheme that it can yield the exactly divergence-free magnetic field and current density on the discrete level. The unique solvability and unconditional stability of the scheme are also proved rigorously. By utilizing the energy argument, error estimates for the velocity, magnetic field and magnetic vector potential are further demonstrated under the low regularity hypothesis for the exact solutions. Numerical results are provided to verify the theoretical analysis and to show the effectiveness of the proposed scheme.

1. INTRODUCTION

The incompressible MHD system models the dynamic behaviors of an electrically conducting fluid under the influence of an external magnetic field. It couples the incompressible Navier–Stokes equations and the Maxwell's equations *via* the Lorentz force and the Ohm's law. There are lots of related applications in different fields, such as astrophysics, engineering related to liquid metal, controlled thermonuclear fusion. Theoretical analysis and mathematical modeling of the MHD equations can be found in [9, 14] and the references therein.

Let Ω be a simply connected bounded domain with Lipschitz-continuous boundary $\Gamma := \partial\Omega$ in $\mathbb{R}^3$. In this paper, we consider numerical approximation of the following incompressible MHD equations:

$$\rho(\boldsymbol{u}_t + \boldsymbol{u} \cdot \nabla\boldsymbol{u}) - \eta\Delta\boldsymbol{u} + \nabla p - \boldsymbol{J} \times \boldsymbol{B} = \boldsymbol{0} \qquad \text{in} \quad \Omega \times J, \tag{1a}$$

[1] Henan Academy of Big Data, Zhengzhou University, Zhengzhou 450052, P.R. China.

[2] School of Mathematics and Statistics, Zhengzhou University, Zhengzhou 450001, P.R. China.

[3] Key Laboratory of Computing and Stochastic Mathematics (Ministry of Education), School of Mathematics and Statistics, Hunan Normal University, Changsha, Hunan 410081, P.R. China.

[4] College of Mathematics and System Sciences, Xinjiang University, Urumqi 830046, P.R. China.

*Corresponding author: `shymath@126.com`

$$\boldsymbol{B}_t + \nabla \times \boldsymbol{E} = \boldsymbol{0}, \quad \boldsymbol{J} - \nabla \times \boldsymbol{H} = \boldsymbol{0} \qquad \text{in} \quad \Omega \times J, \tag{1b}$$

$$\text{div}\boldsymbol{u} = 0, \quad \text{div}\boldsymbol{B} = 0 \qquad \text{in} \quad \Omega \times J, \tag{1c}$$

$$\boldsymbol{B} = \mu\boldsymbol{H}, \quad \boldsymbol{J} = \sigma(\boldsymbol{E} + \boldsymbol{u} \times \boldsymbol{B}) \qquad \text{in} \quad \Omega \times J, \tag{1d}$$

where $T > 0$ is the final time, $J = (0, T]$, ρ is the density of fluid, $\boldsymbol{u}$ is the velocity of fluid, p is the pressure, $\boldsymbol{H}$ is the magnetic field, $\boldsymbol{B}$ is the magnetic induction, $\boldsymbol{J}$ is the current density, and $\boldsymbol{E}$ is the electric field. The physical parameters are the dynamic viscosity η, the magnetic permeability μ and the electric conductivity σ. In this paper, we consider the following initial and boundary conditions,

$$\boldsymbol{u}(\boldsymbol{x}, 0) = \boldsymbol{u}_0(\boldsymbol{x}), \quad \boldsymbol{B}(\boldsymbol{x}, 0) = \boldsymbol{B}_0(\boldsymbol{x}) \qquad \text{in} \quad \Omega,$$

$$\boldsymbol{u} = \boldsymbol{0}, \quad \boldsymbol{B} \times \boldsymbol{n} = \boldsymbol{0} \qquad \text{on} \quad \Gamma \times J,$$

where the initial values satisfy $\nabla \cdot \boldsymbol{u}_0 = \nabla \cdot \boldsymbol{B}_0 = 0$ and $\boldsymbol{n}$ is the unit outer normal vector on Γ.

Recently, divergence-free finite element methods have attracted more and more interest in numerical solving the MHD equations. As for the MHD model in (1), there are three divergence-free constraints to be satisfied. The first constraint is div$\boldsymbol{u} = 0$, that is, the mass conservation of fluid. From [12, 25], when the numerical methods lack of point-wise impressibility, they may introduce a pressure-dependent consistency error which can potentially pollute the computed velocity. Under certain extreme situations, they can lead to spurious results and compromise the fundamental invariant property of incompressible flows. Cockburn *et al.* [5] proposed and analyzed a class of discontinuous Galerkin methods for the incompressible Navier–Stokes equations yielding exactly divergence-free solutions, in which the velocity is approximated by face finite element spaces. Based on this work, Greif *et al.* [16] proposed a mixed DG finite element method for the stationary MHD model.

The next constraint is the divergence-free condition of $\boldsymbol{B}$. It is well-known that it is a precise physical law in electromagnetism which implies that there is no monopole of magnet. From [4, 8, 37], the violation of the divergence-free condition on the discrete level will introduce a strong non-physical force and small perturbations to this condition can lead to large errors in numerical simulation. In the literature, the divergence-free constraint condition for $\boldsymbol{B}$ is relaxed by adding a grad-div augmented term $-\nabla\nabla \cdot \boldsymbol{B}$ [17, 19, 42] or a Lagrange multiplier $r \in H^1$ [13, 34, 36, 41] to numerical formulations. By doing so, the discrete magnetic induction $\boldsymbol{B}_h$ is only weakly divergence-free in the best case. In [23], Hu *et al.* proposed a magnetic-electric based MHD model where the electric field $\boldsymbol{E}$ is kept and regarded as an independent variable. By doing so, div$\boldsymbol{B}_h = 0$ is ensured exactly and directly by using mixed finite element methods together with techniques from finite element exterior calculus. Later, Hiptmair *et al.* [22] proposed a fully divergence-free method for the incompressible MHD system by introducing a new vector potential formulation. For the MHD vector potential model, the constraint condition for $\boldsymbol{B}$ is kept exactly by the definition, $\boldsymbol{B}_h := \mathbf{curl}\,\boldsymbol{A}_h$. We also refer to the review paper [37] and the references therein to other approaches.

The last constraint is div$\boldsymbol{J} = 0$, which is obtained by taking divergence of the ampere equation $\boldsymbol{J} = \mathbf{curl}\,\boldsymbol{H}$. Physically, this condition means that the charge is conservative. In addition, it also plays an important role in keeping the calculation accuracy for the numerical simulation [26, 31, 32]. For the $\boldsymbol{B}$-based MHD model, the discrete current density is exactly divergence-free naturally as a consequence of $\boldsymbol{J}_h := \mathbf{curl}\,\boldsymbol{B}_h$. For the inductionless MHD model, the current density $\boldsymbol{J}$ is a primitive variable and the divergence-free constraint on it can be satisfied either by post-processing [32, 33] or mixed finite element methods in $\boldsymbol{H}(\text{div}, \Omega) \times L^2(\Omega)$ [27, 28, 38–40]. We refer to [26, 29] for further arguments for the importance of the three divergence-free conditions.

Based on the discussion carried out in the previous paragraphs, it is a challenging but interesting work to develop stable numerical schemes which satisfies the three divergence-free conditions simultaneously. Recently, Li *et al.* [29] utilized the potential-based method and constrained transport method to propose a stable finite element method for stationary incompressible MHD equations, in which the velocity, the current density, and the magnetic induction are exactly divergence-free on the discrete level. Compared with traditional potential-based and CT methods, the new method treats magnetic field $\boldsymbol{H}$ and magnetic vector potential $\boldsymbol{A}$ as individual variables by means of edge finite element discretization. The discrete current density $\boldsymbol{J}_h := \mathbf{curl}\,\boldsymbol{H}_h$ and the

discrete magnetic induction $\boldsymbol{B}_h := \mathbf{curl}\,\boldsymbol{A}_h$ are divergence-free naturally. To fulfill the divergence-free constraint on $\boldsymbol{u}$, they approximated the velocity by combing divergence-conforming finite element spaces with DG approach. Here and afterwards, we refer to this system simply as CT-MHD model. The motivation of this work is to extend the divergence-free finite element method to the non-stationary setting. For the sake of simplicity, we are mainly concerned with the divergence-free constraints on $\boldsymbol{B}$ and $\boldsymbol{J}$.

The purpose of this paper is to present and analyze a fully discrete finite element method for the non-stationary CT-MHD system. The finite element approximation is based on mixed finite elements, where fluid stable elements are used for the Navier–Stokes equations, $\boldsymbol{H}(\mathbf{curl})$-conforming edge elements are used for the magnetic equation and magnetic vector potential equations. For the temporal discretization, we use a semi-implicit Euler scheme. At each time step, the fully discrete scheme is linear in the implementation and the magnetic vector potential is solved separately from the whole system. As a result, the proposed scheme ensures the exactly divergence-free approximation of the magnetic induction and current density. Moreover, we prove that the scheme is uni-solvent and unconditionally energy stable. Under the low regularity hypothesis for the exact solutions, we utilize the energy argument to establish the error estimates for the velocity, magnetic field and magnetic vector potential. A series of numerical tests are carried out to confirm our theoretical results and verify the performance of the scheme.

Here we would like to specify the main differences between this paper and the most relevant [22,29]. On the one hand, compared to the work in [22], they only used the magnetic vector potential as the variable, then the magnetic field and current density are defined by $\boldsymbol{B} := \mathbf{curl}\,\boldsymbol{A}$ and $\boldsymbol{J} := -\boldsymbol{A}_t + \boldsymbol{u} \times \boldsymbol{B}$. Thus, the scheme therein only can yield the exactly divergence-free magnetic field on the discrete level. While our scheme can ensure the exactly divergence-free approximation of the magnetic induction and current density. In addition, there is a little different in guaranteeing the uniqueness of the magnetic vector potential. They use the temporal gauge while we adopt the Coulomb's gauge. What's more, they only provide a plain convergence for the finite element solutions and no error estimates are given. On the other hand, compared to the work in [29], they focused stable finite element discretization for stationary incompressible MHD equations and corresponding fast solvers. Although some convergence results of the finite element solution are established, no error analysis are presented. It is much more complicated and difficult to carry out the error analysis as we have to deal with the issues due to the nonlinear coupling of multiple variables. Therefore, more delicate analyses are needed for the error estimates.

The paper is organized as follows. In Section 2, we introduce some notations and present the energy estimate fo the MHD equations. In Section 3, we propose a fully discrete finite element method for the MHD equations. In Section 4, we state the main results of this work. In Section 5, we deduce some detailed proofs in Section 4. In Section 6, we present some numerical experiments to confirm the stability and accuracy of the scheme. In Section 7, we conclude with a few remarks.

2. Preliminaries

We start by introducing some notations and Sobolev spaces. Throughout the paper, the vector-valued functions and vector-valued function spaces in $\mathbb{R}^3$ are denoted in boldface. As usual, the inner product and norm in $L^2(\Omega)$ are denoted by $(\cdot, \cdot)$ and $\|\cdot\|$, respectively. Let $W^{m,p}(\Omega)$ stand for the standard Sobolev spaces equipped with the standard Sobolev norms $\|\cdot\|_{m,p}$. For $p = 2$, we write $H^m(\Omega)$ for $W^{m,2}(\Omega)$ and its corresponding norm is $\|\cdot\|_m$. For a given Sobolev space X, we write $L^q(0, T; X)$ for the Bochner space. We will use the following notations for some spaces,

$$\boldsymbol{H}_0^1(\Omega) = \left\{ \boldsymbol{v} \in \boldsymbol{H}^1(\Omega), \, \boldsymbol{v}|_\Gamma = \boldsymbol{0} \right\}, \, L_0^2(\Omega) = \left\{ q \in L^2(\Omega), \int_\Omega q \, \mathrm{d}\boldsymbol{x} = 0 \right\},$$

$$\boldsymbol{H}(\mathbf{curl}, \Omega) = \left\{ \boldsymbol{C} \in \boldsymbol{L}^2(\Omega), \mathbf{curl}\,\boldsymbol{C} \in \boldsymbol{L}^2(\Omega) \right\},$$

$$\boldsymbol{H}_0(\mathbf{curl}, \Omega) = \left\{ \boldsymbol{C} \in \boldsymbol{H}(\mathbf{curl}, \Omega), \boldsymbol{n} \times \boldsymbol{C}|_\Gamma = \boldsymbol{0} \right\}.$$

In addition, the standard norm in $\boldsymbol{H}(\mathbf{curl}, \Omega)$ is denoted by $\|\cdot\|_{\mathbf{curl}}$. Here and what follows, we use C to denote generic positive constants independent of the discretization parameters, which may take different values at different places.

Then we present the CT-MHD model in a dimensionless form. Since $\mathrm{div}\,\boldsymbol{B} = 0$ in Ω and $\boldsymbol{B} \times \boldsymbol{n} = \boldsymbol{0}$ on Γ, we invoke with the vector potential theorem in [15] to introduce a magnetic vector potential $\boldsymbol{A}$ with the Coulomb's gauge such that

$$\boldsymbol{B} = \mathbf{curl}\,\boldsymbol{A}, \quad \mathrm{div}\,\boldsymbol{A} = 0 \qquad \text{in} \quad \Omega, \tag{2}$$

$$\boldsymbol{A} \cdot \boldsymbol{n} = 0, \quad \mathbf{curl}\,\boldsymbol{A} \times \boldsymbol{n} = \boldsymbol{0} \qquad \text{on} \quad \Gamma. \tag{3}$$

Putting (2) into (1) and eliminating $\boldsymbol{J}$ and $\boldsymbol{E}$, we can obtain the following CT-MHD model

$$\rho(\boldsymbol{u}_t + \boldsymbol{u} \cdot \nabla \boldsymbol{u}) - \eta \Delta \boldsymbol{u} + \nabla p - \mathbf{curl}\,\boldsymbol{H} \times \mathbf{curl}\,\boldsymbol{A} = \boldsymbol{0} \qquad \text{in} \quad \Omega \times J, \tag{4a}$$

$$(\mu \boldsymbol{H})_t + \mathbf{curl}\left(\sigma^{-1}\mathbf{curl}\,\boldsymbol{H}\right) + \mathbf{curl}\left(\mathbf{curl}\,\boldsymbol{A} \times \boldsymbol{u}\right) = \boldsymbol{0} \qquad \text{in} \quad \Omega \times J, \tag{4b}$$

$$\mathbf{curl}\left(\mu^{-1}\mathbf{curl}\,\boldsymbol{A}\right) - \mathbf{curl}\,\boldsymbol{H} = \boldsymbol{0} \qquad \text{in} \quad \Omega \times J, \tag{4c}$$

$$\mathrm{div}\,\boldsymbol{u} = 0, \quad \mathrm{div}(\mu \boldsymbol{H}) = 0, \quad \mathrm{div}\,\boldsymbol{A} = 0 \qquad \text{in} \quad \Omega \times J. \tag{4d}$$

The system are complemented with the following initial and boundary conditions,

$$\boldsymbol{u}(\boldsymbol{x}, 0) = \boldsymbol{u}_0(\boldsymbol{x}), \quad \boldsymbol{H}(\boldsymbol{x}, 0) = \boldsymbol{H}_0(\boldsymbol{x}) \qquad \text{in} \quad \Omega,$$

$$\boldsymbol{u} = \boldsymbol{0}, \quad \boldsymbol{H} \times \boldsymbol{n} = \boldsymbol{0}, \quad \boldsymbol{A} \cdot \boldsymbol{n} = 0, \quad \mathbf{curl}\,\boldsymbol{A} \times \boldsymbol{n} = \boldsymbol{0} \qquad \text{on} \quad \Gamma \times J,$$

where the initial values satisfy $\nabla \cdot \boldsymbol{u}_0 = \nabla \cdot \boldsymbol{H}_0 = 0$.

Let $L, t_0, H_0, u_0 = L/t_0$ be characteristic quantities of length, time, magnetic field, and fluid velocity, respectively. We introduce the dimensionless variables as follows

$$\boldsymbol{x} \leftarrow \boldsymbol{x}/L, \, t \leftarrow t/t_0, \, \boldsymbol{u} \leftarrow \boldsymbol{u}/u_0, \, p \leftarrow p/\left(\rho u_0^2\right), \, \boldsymbol{H} \leftarrow \boldsymbol{H}/H_0, \, \boldsymbol{A} \leftarrow \boldsymbol{A}/(\mu H_0 L).$$

Then, the MHD system (4) can be written in a dimensionless form,

$$\boldsymbol{u}_t + \boldsymbol{u} \cdot \nabla \boldsymbol{u} - R_e^{-1}\Delta \boldsymbol{u} + \nabla p - \kappa \mathbf{curl}\,\boldsymbol{H} \times \mathbf{curl}\,\boldsymbol{A} = \boldsymbol{0} \qquad \text{in} \quad \Omega \times J, \tag{5a}$$

$$\mathrm{div}\,\boldsymbol{u} = 0 \qquad \text{in} \quad \Omega \times J, \tag{5b}$$

$$\boldsymbol{H}_t + R_m^{-1}\mathbf{curl}\,\mathbf{curl}\,\boldsymbol{H} + \mathbf{curl}\left(\mathbf{curl}\,\boldsymbol{A} \times \boldsymbol{u}\right) = \boldsymbol{0} \qquad \text{in} \quad \Omega \times J, \tag{5c}$$

$$\mathrm{div}\,\boldsymbol{H} = 0 \qquad \text{in} \quad \Omega \times J, \tag{5d}$$

$$\mathbf{curl}\,\mathbf{curl}\,\boldsymbol{A} - \mathbf{curl}\,\boldsymbol{H} + \nabla \phi = \boldsymbol{0} \qquad \text{in} \quad \Omega \times J, \tag{5e}$$

$$\mathrm{div}\,\boldsymbol{A} = 0 \qquad \text{in} \quad \Omega \times J, \tag{5f}$$

$$\boldsymbol{u}(\boldsymbol{x}, 0) = \boldsymbol{u}_0(\boldsymbol{x}), \quad \boldsymbol{H}(\boldsymbol{x}, 0) = \boldsymbol{H}_0(\boldsymbol{x}) \qquad \text{in} \quad \Omega, \tag{5g}$$

$$\boldsymbol{u} = \boldsymbol{0}, \quad \boldsymbol{H} \times \boldsymbol{n} = \boldsymbol{0}, \quad \boldsymbol{A} \cdot \boldsymbol{n} = 0, \quad \mathbf{curl}\,\boldsymbol{A} \times \boldsymbol{n} = \boldsymbol{0}, \quad \nabla \phi \cdot \boldsymbol{n} = 0 \qquad \text{on} \quad \Gamma \times J, \tag{5h}$$

where $R_e = \rho L u_0/\eta$ is the Reynolds number, $R_m = \mu \sigma L u_0$ is the magnetic Reynolds number and $\kappa = \mu H_0^2/\left(\rho u_0^2\right)$ is the coupling number between the fluid and the magnetic field. Note that we have introduced a Lagrange multiplier ϕ with homogeneous Neumann boundary condition to deal with divergence-free constraint of $\mathrm{div}\,\boldsymbol{A} = 0$. Indeed, the equation (5e) is equivalent to the following equation

$$\mathbf{curl}\,\mathbf{curl}\,\boldsymbol{A} - \mathbf{curl}\,\boldsymbol{H} = \boldsymbol{0} \quad \text{in} \quad \Omega \times J.$$

This is because if we apply divergence operator to (5e), we get $\Delta \phi = 0$. From the boundary condition for ϕ, we deduce $\phi = 0$ in $H^1/\mathbb{R}$. In this paper, we adopt (5e) since this formulation allows us easily deal with the divergence-free condition for $\boldsymbol{A}$. Similar ideas can be found in [29, 36].

Now we derive a weak formulation of (5). For convenience, we introduce some notations for function spaces

$$\boldsymbol{V} := \boldsymbol{H}_0^1(\Omega), \quad Q := L_0^2(\Omega), \quad \boldsymbol{W} := \boldsymbol{H}_0(\mathbf{curl}, \Omega), \quad \boldsymbol{D} := \boldsymbol{H}(\mathbf{curl}, \Omega), \quad S := H^1(\Omega)/\mathbb{R}.$$

With the above notations, a weak formulation of (5) amounts to finding $(\boldsymbol{u}, p, \boldsymbol{H}, \boldsymbol{A}, \phi) \in \boldsymbol{V} \times Q \times \boldsymbol{W} \times \boldsymbol{D} \times S$ such that for all $(\boldsymbol{v}, q, \boldsymbol{C}, \boldsymbol{M}, \psi) \in \boldsymbol{V} \times Q \times \boldsymbol{W} \times \boldsymbol{D} \times S$,

$$(\boldsymbol{u}_t, \boldsymbol{v}) + R_e^{-1}(\nabla \boldsymbol{u}, \nabla \boldsymbol{v}) + (\boldsymbol{u} \cdot \nabla \boldsymbol{u}, \boldsymbol{v}) - (p, \mathrm{div}\boldsymbol{v}) - \kappa(\mathbf{curl}\,\boldsymbol{H} \times \mathbf{curl}\,\boldsymbol{A}, \boldsymbol{v}) = 0, \tag{6a}$$

$$(\mathrm{div}\boldsymbol{u}, q) = 0, \tag{6b}$$

$$(\boldsymbol{H}_t, \boldsymbol{C}) + R_m^{-1}(\mathbf{curl}\,\boldsymbol{H}, \mathbf{curl}\,\boldsymbol{C}) + (\mathbf{curl}\,\boldsymbol{A} \times \boldsymbol{u}, \mathbf{curl}\,\boldsymbol{C}) = 0, \tag{6c}$$

$$(\mathbf{curl}\,\boldsymbol{A}, \mathbf{curl}\,\boldsymbol{M}) + (\nabla \phi, \boldsymbol{M}) - (\boldsymbol{H}, \mathbf{curl}\,\boldsymbol{M}) = 0, \tag{6d}$$

$$(\boldsymbol{A}, \nabla \psi) = 0. \tag{6e}$$

Note that there is no explicit equation on the divergence-free constraint of $\boldsymbol{H}$ in the above weak formulation. This constraint is implied by (6c), provided that the initial value $\boldsymbol{H}_0$ is divergence-free. More specifically, since $\nabla r \in \boldsymbol{W}$ for all $r \in H_0^1(\Omega)$, we can choose $\boldsymbol{C} = \nabla r$ in (6c) to deduce $(\boldsymbol{H}_t, \nabla r) = 0$. Invoking with the orthogonal decomposition in $\boldsymbol{L}^2(\Omega)$ [15], we conclude that $\mathrm{div}\boldsymbol{H}_t = 0$. Thus, when the initial value of magnetic filed satisfies $\mathrm{div}\boldsymbol{H}_0 = 0$, then $\mathrm{div}\boldsymbol{H}(t) = 0$, for all $t \in (0, T]$.

To end this section, we give the basic formal energy estimates for the model (5).

Theorem 2.1. *Let $(\boldsymbol{u}, p, \boldsymbol{H}, \boldsymbol{A}, \phi)$ be the solution of* (6), *the following energy law holds*

$$\frac{\mathrm{d}}{\mathrm{d}t}\left(\frac{1}{2}\|\boldsymbol{u}\|^2 + \frac{\kappa}{2}\|\boldsymbol{H}\|^2\right) + R_e^{-1}\|\nabla \boldsymbol{u}\|^2 + \kappa R_m^{-1}\|\mathbf{curl}\,\boldsymbol{H}\|^2 = 0. \tag{7}$$

Moreover, we have

$$\|\mathbf{curl}\,\boldsymbol{A}\| \leq \|\boldsymbol{H}\|. \tag{8}$$

Proof. By taking $(\boldsymbol{v}, q) = (\boldsymbol{u}, p)$ in (6a) and (6b), and using $(\boldsymbol{u} \cdot \nabla \boldsymbol{u}, \boldsymbol{u}) = 0$, we get

$$\frac{1}{2}\frac{\mathrm{d}}{\mathrm{d}t}\|\boldsymbol{u}\|^2 + R_e^{-1}\|\nabla \boldsymbol{u}\|^2 - \kappa(\mathbf{curl}\,\boldsymbol{H} \times \mathbf{curl}\,\boldsymbol{A}, \boldsymbol{u}) = 0. \tag{9}$$

By taking $\boldsymbol{C} = \kappa \boldsymbol{H}$ in (6c), we have

$$\frac{\kappa}{2}\frac{\mathrm{d}}{\mathrm{d}t}\|\boldsymbol{H}\|^2 + \kappa R_m^{-1}\|\mathbf{curl}\,\boldsymbol{H}\|^2 + \kappa(\mathbf{curl}\,\boldsymbol{A} \times \boldsymbol{u}, \mathbf{curl}\,\boldsymbol{H}) = 0. \tag{10}$$

Hence, by combining (9) and (10), we obtain the law of energy dissipation (7).

Furthermore, by taking $(\boldsymbol{M}, \psi) = (\boldsymbol{A}, \phi)$ in (6d) and (6e) and using Cauchy–Schwarz inequality, we arrive at

$$\|\mathbf{curl}\,\boldsymbol{A}\|^2 = (\boldsymbol{H}, \mathbf{curl}\,\boldsymbol{A}) \leq \|\boldsymbol{H}\|\|\mathbf{curl}\,\boldsymbol{A}\|,$$

which indicates that the desired result (8) holds. □

On the one hand, we note that the energy law describes the variation of the total energy caused by energy conversion. The total energy consists of the fluid kinetic energy $\frac{1}{2}\|\boldsymbol{u}\|^2$ and the magnetic field energy $\frac{\kappa}{2}\|\boldsymbol{H}\|^2$. The dissipation stems from the friction losses $R_e^{-1}\|\nabla \boldsymbol{u}\|^2$ and the Ohmic losses $\kappa R_m^{-1}\|\mathbf{curl}\,\boldsymbol{H}\|^2$. On the other hand, we see that there is no term related to the magnetic vector potential $\boldsymbol{A}$ in the energy law. This observation indicates that $\boldsymbol{A}$ is only a intermediate variable in this system. Even so, we still have some stability results for it.

Remark 2.2. Note that the boundary we considered for the magnetic induction and electric field is $\boldsymbol{B} \times \boldsymbol{n} = \boldsymbol{0}$ and $\boldsymbol{E} \cdot \boldsymbol{n} = 0$. As to another frequently used set of boundary conditions for the magnetic induction and electric field, $\boldsymbol{B} \cdot \boldsymbol{n} = 0$ and $\boldsymbol{E} \times \boldsymbol{n} = \boldsymbol{0}$, we need make some modifications on the boundary conditions for the magnetic field and magnetic vector potential. Invoking with the vector potential theorem in [15], we deduce the following boundary conditions for $\boldsymbol{H}$ and $\boldsymbol{A}$,

$$\boldsymbol{H} \cdot \boldsymbol{n} = 0, \quad \mathbf{curl}\, \boldsymbol{H} \times \boldsymbol{n} = \boldsymbol{0}, \quad \boldsymbol{A} \times \boldsymbol{n} = \boldsymbol{0} \quad \text{on} \quad \Gamma \times J.$$

Furthermore, our forthcoming analysis can be easily extended to this type boundary conditions.

3. A SEMI-IMPLICIT MIXED FEM

This section is devoted to giving the fully discrete finite element scheme for the MHD equations. For the space discretization, let $\mathcal{T}_h$ be a quasi-uniform and shape-regular tetrahedral mesh of Ω. As usual, we introduce the local mesh size $h_K = \text{diam}(K)$ and the global mesh size $h := \max_{K \in \mathcal{T}_h} h_K$. For any integer $k \geq 0$, let $P_k(K)$ be the space of polynomials of degree k on element K and define $\boldsymbol{P}_k(K) = P_k(K)^3$. To approximate the velocity and pressure $(\boldsymbol{u}, p)$, we use the conforming finite element pair $(\boldsymbol{V}_h \times Q_h) \subset (\boldsymbol{V} \times Q)$, which satisfies the discrete inf-sup condition,

$$\inf_{0 \neq q_h \in Q_h} \sup_{\boldsymbol{0} \neq \boldsymbol{v}_h \in \boldsymbol{V}_h} \frac{(q_h, \text{div}\boldsymbol{v}_h)}{\|\nabla \boldsymbol{v}_h\| \|q_h\|} \geq \beta_s, \tag{11}$$

where β_s is a constant independent of mesh size h. To approximate the magnetic field $\boldsymbol{H}$, we employ the conforming finite element space $\boldsymbol{W}_h \subset \boldsymbol{W}$. To approximate the magnetic vector potential and Lagrange multiplier $(\boldsymbol{A}, \phi)$, we adopt the conforming finite element pair $(\boldsymbol{D}_h \times S_h) \subset (\boldsymbol{D} \times S)$, which satisfies the discrete inf-sup condition,

$$\inf_{0 \neq \psi_h \in S_h} \sup_{\boldsymbol{0} \neq \boldsymbol{M}_h \in \boldsymbol{D}_h} \frac{(\nabla \psi_h, \boldsymbol{M}_h)}{\|\psi_h\|_1 \|\boldsymbol{M}_h\|_{\mathbf{curl}}} \geq \beta_m, \tag{12}$$

where β_m is a constant independent of mesh size h. We assume that the finite element spaces possess the following approximation properties ulteriorly. There exists an integer $k \geq 1$ such that the following standard approximation properties hold for $k \geq 1$,

$$\inf_{\boldsymbol{v}_h \in \boldsymbol{V}_h} (\|\boldsymbol{u} - \boldsymbol{v}_h\| + h\|\nabla(\boldsymbol{u} - \boldsymbol{v}_h)\|) \leq Ch^{k+1} \|\boldsymbol{u}\|_{k+1}, \tag{13}$$

$$\inf_{\boldsymbol{C}_h \in \boldsymbol{W}_h} (\|\boldsymbol{H} - \boldsymbol{C}_h\| + \|\mathbf{curl}(\boldsymbol{H} - \boldsymbol{C}_h)\|) \leq Ch^k (\|\boldsymbol{H}\|_k + \|\mathbf{curl}\,\boldsymbol{H}\|_k), \tag{14}$$

$$\inf_{\boldsymbol{M}_h \in \boldsymbol{D}_h} (\|\boldsymbol{A} - \boldsymbol{M}_h\| + \|\mathbf{curl}(\boldsymbol{A} - \boldsymbol{M}_h)\|) \leq Ch^k (\|\boldsymbol{A}\|_k + \|\mathbf{curl}\,\boldsymbol{A}\|_k), \tag{15}$$

$$\inf_{q_h \in Q_h} \|p - q_h\|_k \leq Ch^k \|p\|_k, \quad \inf_{\psi_h \in S_h} (\|\phi - \psi_h\| + h\|\nabla(\phi - \psi_h)\|) \leq Ch^{k+1} \|\phi\|_{k+1}. \tag{16}$$

Many existing stable finite element pairs can be available in present setting [3, 15, 30]. In the numerical experiments of Section 6, we choose Mini-element to discrete the velocity and pressure, the lowest order Nédélec edge element for the magnetic field and magnetic vector potential, and linear nodal element for the Lagrange multiplier. To be specific,

$$\begin{aligned}
\boldsymbol{V}_h &= \{\boldsymbol{v}_h \in \boldsymbol{V} : \boldsymbol{v}_h|_K \in \boldsymbol{P}_{1,b}(K), \quad \forall K \in \mathcal{T}_h\}, \\
Q_h &= \{q_h \in H^1(\Omega) : q_h|_K \in P_1(K), \quad \forall K \in \mathcal{T}_h\} \cap Q, \\
\boldsymbol{W}_h &= \{\boldsymbol{C}_h \in \boldsymbol{W} : \boldsymbol{C}_h|_K \in \boldsymbol{P}_0(K) + \boldsymbol{P}_0(K) \times \boldsymbol{x}, \quad \forall K \in \mathcal{T}_h\}, \\
\boldsymbol{D}_h &= \{\boldsymbol{M}_h \in \boldsymbol{D} : \boldsymbol{M}_h|_K \in \boldsymbol{P}_0(K) + \boldsymbol{P}_0(K) \times \boldsymbol{x}, \quad \forall K \in \mathcal{T}_h\}, \\
S_h &= \{\psi_h \in H^1(\Omega) : \psi_h|_K \in P_1(K), \quad \forall K \in \mathcal{T}_h\}
\end{aligned} \tag{17}$$

where $P_{1,b}(K) = P_1(K) \oplus \text{span}\{\lambda_1 \lambda_2 \lambda_3 \lambda_4\}$, λ_i, $i = 1, 2, 3, 4$ are the barycentric coordinate functions on K.

For convenience, we define the discrete kernel space of the divergence operator on $\boldsymbol{V}_h$ by

$$\boldsymbol{V}_h^0 = \{\boldsymbol{v}_h \in \boldsymbol{V}_h, \quad (\mathrm{div}\boldsymbol{v}_h, q_h) = 0, \quad \forall q_h \in Q_h\}.$$

Similarly, we introduce the discretely solenoidal function space on $\boldsymbol{D}_h$ by

$$\boldsymbol{D}_h^0 = \{\boldsymbol{M}_h \in \boldsymbol{D}_h, \quad (\boldsymbol{M}_h, \nabla\psi_h) = 0, \quad \forall \psi_h \in S_h\}.$$

From the de-Rham sequence, we know that there exists a Lagrange finite element space $R_h \subset H_0^1(\Omega)$ such that $\nabla R_h \subset \boldsymbol{W}_h$. For the choice of (17),

$$R_h = \left\{s_h \in H_0^1(\Omega) : s_h|_K \in P_1(K), \quad \forall K \in \mathcal{T}_h\right\}.$$

Then the discretely solenoidal function space on $\boldsymbol{W}_h$ is defined by

$$\boldsymbol{W}_h^0 = \{\boldsymbol{C}_h \in \boldsymbol{W}_h, \quad (\boldsymbol{C}_h, \nabla r_h) = 0, \quad \forall r_h \in R_h\}.$$

Further, there holds the following Poincaré's inequality [1, 18, 21, 34, 36],

$$\|\boldsymbol{C}_h\|_{\mathbf{curl}} \leq C_*\|\mathbf{curl}\,\boldsymbol{C}_h\|, \quad \forall \boldsymbol{C}_h \in \boldsymbol{D}_h^0 \cup \boldsymbol{W}_h^0. \tag{18}$$

In order to deal with the convection term in (5a), we define the following trilinear form

$$\mathcal{O}(\boldsymbol{u}, \boldsymbol{v}, \boldsymbol{w}) = \frac{1}{2}((\boldsymbol{u} \cdot \nabla\boldsymbol{v}, \boldsymbol{w}) - (\boldsymbol{u} \cdot \nabla\boldsymbol{w}, \boldsymbol{v})) \quad \forall \boldsymbol{u}, \boldsymbol{v}, \boldsymbol{w} \in \boldsymbol{V}.$$

For the time discretization, let $\{t_n = n\tau : n = 0, 1, \cdots, N\}, \tau = T/N$, be an equidistant partition of the time interval $[0, T]$. Given a function $\omega(x, t)$, the full discrete approximation to $\omega(x, t_n)$ will be denoted by ω_h^n. For $n \geq 1$ and any function v, define $\delta_t v^n = \frac{v^n - v^{n-1}}{\tau}$.

With the discrete spaces and above notions, a fully discrete finite element scheme for problem (5) reads as follows. For any $n \geq 1$, we find $(\boldsymbol{u}_h^n, p_h^n, \boldsymbol{H}_h^n, \boldsymbol{A}_h^n, \phi_h^n) \in \boldsymbol{V}_h \times Q_h \times \boldsymbol{W}_h \times \boldsymbol{D}_h \times S_h$ such that for all $(\boldsymbol{v}_h, q_h, \boldsymbol{C}_h, \boldsymbol{M}_h, \psi_h) \in \boldsymbol{V}_h \times Q_h \times \boldsymbol{W}_h \times \boldsymbol{D}_h \times S_h$,

$$(\delta_t\boldsymbol{u}_h^n, \boldsymbol{v}_h) + R_e^{-1}(\nabla\boldsymbol{u}_h^n, \nabla\boldsymbol{v}_h) + \mathcal{O}(\boldsymbol{u}_h^{n-1}, \boldsymbol{u}_h^n, \boldsymbol{v}_h) - (p_h^n, \mathrm{div}\boldsymbol{v}_h) - \kappa(\mathbf{curl}\,\boldsymbol{H}_h^n \times \mathbf{curl}\,\boldsymbol{A}_h^n, \boldsymbol{v}_h) = 0, \tag{19a}$$

$$(\mathrm{div}\boldsymbol{u}_h^n, q_h) = 0, \tag{19b}$$

$$(\delta_t\boldsymbol{H}_h^n, \boldsymbol{C}_h) + R_m^{-1}(\mathbf{curl}\,\boldsymbol{H}_h^n, \mathbf{curl}\,\boldsymbol{C}_h) + (\mathbf{curl}\,\boldsymbol{A}_h^n \times \boldsymbol{u}_h^n, \mathbf{curl}\,\boldsymbol{C}_h) = 0, \tag{19c}$$

$$(\mathbf{curl}\,\boldsymbol{A}_h^n, \mathbf{curl}\,\boldsymbol{M}_h) + (\nabla\phi_h^n, \boldsymbol{M}_h) - (\boldsymbol{H}_h^{n-1}, \mathbf{curl}\,\boldsymbol{M}_h) = 0, \tag{19d}$$

$$(\boldsymbol{A}_h^n, \nabla\psi_h) = 0. \tag{19e}$$

At the initial time step, $\boldsymbol{u}_h^0 = \mathcal{P}_h\boldsymbol{u}_0$ and $\boldsymbol{H}_h^0 = \mathcal{F}_h\boldsymbol{H}_0$, where $\mathcal{P}_h$ and $\mathcal{F}_h$ are projection operators defined in Section 5. Finally, we give several remarks concerning the proposed scheme.

Remark 3.1. From (19e), we know that the discrete magnetic vector potential is divergence-free weakly. In fact, the discrete solution for the magnetic field also satisfies the weakly divergence free property. For any $r_h \in R_h$, by taking $\boldsymbol{C}_h = \nabla r_h$ in (19c), we obtain $(\delta_t\boldsymbol{H}_h^n, \nabla r_h) = 0$, namely, $\left((\boldsymbol{H}_h^n - \boldsymbol{H}_h^{n-1})/\tau, \nabla r_h\right) = 0$. Combing with $(\boldsymbol{H}_h^0, \nabla r_h) = 0$, it is inferred that $(\boldsymbol{H}_h^n, \nabla r_h) = 0$ for $n = 0, 1, \cdots, N$. Thus, we do not need to add a Lagrange multiplier in the magnetic equation as in [29, 36].

Remark 3.2. After obtaining the magnetic field $\boldsymbol{H}_h^n$ and the magnetic vector potential $\boldsymbol{A}_h^n$, we can define the current density as $\boldsymbol{J}_h^n := \mathbf{curl}\,\boldsymbol{H}_h^n$ and the magnetic induction as $\boldsymbol{B}_h^n := \mathbf{curl}\,\boldsymbol{A}_h^n$. Thus the discrete current density and magnetic induction are divergence-free exactly.

Remark 3.3. Compared with the semi-implicit scheme for the **B**-based model in [13,19], the extra cost is the computation of a saddle problem for the magnetic vector potential and Lagrange multiplier at each time step. Moreover, we have decoupling them from other variables by lagging the magnetic field in (19d), which makes the implementation simpler and the scheme more efficient. In the future, we will consider using the regularization strategy proposed in [11] with $\epsilon = \tau$ to remove the Lagrangian multiplier ϕ for the magnetic vector potential **A** while keeping the numerical accuracy.

Remark 3.4. As for the detailed implementation process of (19), we can first solve the discrete problem (19d) and (19e) for $(\boldsymbol{A}, \phi)$ and then solve the discrete problem (19a)–(19c) for $(\boldsymbol{u}, p, \boldsymbol{H})$. Thus, there exits a similar fully discrete scheme, whose implementation process is really just the opposite. A brief discussion about this scheme is laid down in Appendix A.

4. MAIN RESULTS

In this section, we state the main results of this paper. First, we establish the unique solvability of the proposed scheme (19) is the following theorem.

Theorem 4.1. *For any $\tau > 0$ and $h > 0$, the proposed scheme (19) is uniquely solvable at each time step.*

Proof. As we stated in Remark 3.4, we can implement the proposed scheme in succession by first solving (19d) and (19e) for $(\boldsymbol{A}_h^n, \phi_h^n)$ and then solving (19a)–(19c) for $(\boldsymbol{u}_h^n, p_h^n, \boldsymbol{H}_h^n)$. Thus, we turn to prove the unique solvability of these two subproblems. For the discrete problem (19d) and (19e), it is linear with respect to the solution $(\boldsymbol{A}_h^n, \phi_h^n)$. Since it is further finite-dimensional, it just requires to prove that the following the homogeneous problem only has zero solution, for all $n \geq 1$ and any $(\boldsymbol{M}_h, \psi_h) \in \boldsymbol{D}_h \times S_h$,

$$(\mathbf{curl}\,\boldsymbol{A}_h^n, \mathbf{curl}\,\boldsymbol{M}_h) + (\nabla \phi_h^n, \boldsymbol{M}_h) = 0, \tag{20a}$$

$$(\boldsymbol{A}_h^n, \nabla \psi_h) = 0. \tag{20b}$$

Taking $(\boldsymbol{M}_h, \psi_h) = (\boldsymbol{A}_h^n, \phi_h^n)$ in (20a)-(20b), we have $\|\mathbf{curl}\,\boldsymbol{A}_h^n\| = 0$. Invoking the Poincaré's inequality in (18), we get $\|\boldsymbol{A}_h^n\| = 0$, which means that $\boldsymbol{A}_h^n = \boldsymbol{0}$. According to the inf-sup condition (12) and (20a), we obtain $\phi_h^n = 0$. Next, we consider the discrete problem (19a)–(19c). Note that, given $\boldsymbol{u}_h^{n-1}$, $\boldsymbol{H}_h^{n-1}$ and $\boldsymbol{A}_h^n$, it is linear with respect to the solution $(\boldsymbol{u}_h^n, p_h^n, \boldsymbol{H}_h^n)$. Similarly, since it is further finite-dimensional, it merely requires to prove that the following the homogeneous problem only has zero solution, for all $n \geq 1$ and any $(\boldsymbol{v}_h, q_h, \boldsymbol{C}_h) \in \boldsymbol{V}_h \times Q_h \times \boldsymbol{W}_h$,

$$\left(\frac{\boldsymbol{u}_h^n}{\tau}, \boldsymbol{v}_h\right) + R_e^{-1}(\nabla \boldsymbol{u}_h^n, \nabla \boldsymbol{v}_h) + \mathcal{O}(\boldsymbol{u}_h^{n-1}, \boldsymbol{u}_h^n, \boldsymbol{v}_h) - (p_h^n, \nabla \cdot \boldsymbol{v}_h) - \kappa(\mathbf{curl}\,\boldsymbol{H}_h^n \times \mathbf{curl}\,\boldsymbol{A}_h^n, \boldsymbol{v}_h) = 0, \tag{21a}$$

$$(\mathrm{div}\,\boldsymbol{u}_h^n, q_h) = 0, \tag{21b}$$

$$\left(\frac{\boldsymbol{H}_h^n}{\tau}, \boldsymbol{C}_h\right) + R_m^{-1}(\mathbf{curl}\,\boldsymbol{H}_h^n, \mathbf{curl}\,\boldsymbol{C}_h) - (\mathbf{curl}\,\boldsymbol{A}_h^n \times \boldsymbol{u}_h^n, \mathbf{curl}\,\boldsymbol{C}_h) = 0. \tag{21c}$$

We take $(\boldsymbol{v}_h, q_h, \boldsymbol{C}_h) = (\boldsymbol{u}_h^n, p_h^n, \kappa \boldsymbol{H}_h^n)$ in (21) to get

$$\frac{\|\boldsymbol{u}_h^n\|^2}{\tau} + R_e^{-1}\|\nabla \boldsymbol{u}_h^n\|^2 = 0, \quad \kappa \frac{\|\boldsymbol{H}_h^n\|^2}{\tau} + \kappa R_m^{-1}\|\mathbf{curl}\,\boldsymbol{H}_h^n\|^2 = 0. \tag{22}$$

Thus, we get $\boldsymbol{u}_h^n = \boldsymbol{H}_h^n = \boldsymbol{0}$. From (11), we deduce that $p_h^n = 0$. This concludes the proof. □

Then, we present the stability of the discrete problem (19) in the following theorem.

Theorem 4.2. *The discrete solution $(\boldsymbol{u}_h^n, p_h^n, \boldsymbol{H}_h^n, \boldsymbol{A}_h^n, \phi_h^n)$ satisfies*

$$\frac{\|\boldsymbol{u}_h^n\|^2 - \|\boldsymbol{u}_h^{n-1}\|^2 + \|\boldsymbol{u}_h^n - \boldsymbol{u}_h^{n-1}\|^2}{2\tau} + \kappa \frac{\|\boldsymbol{H}_h^n\|^2 - \|\boldsymbol{H}_h^{n-1}\|^2 + \|\boldsymbol{H}_h^n - \boldsymbol{H}_h^{n-1}\|^2}{2\tau}$$
$$+ R_e^{-1}\|\nabla\boldsymbol{u}_h^n\|^2 + \kappa R_m^{-1}\|\mathbf{curl}\,\boldsymbol{H}_h^n\|^2 = 0, \tag{23}$$
$$\|\mathbf{curl}\,\boldsymbol{A}_h^n\| \le \|\boldsymbol{H}_h^{n-1}\|. \tag{24}$$

Consequently, we have the following estimates for $m = 1, 2, \cdots, N$,

$$\|\boldsymbol{u}_h^m\|^2 + \kappa\|\boldsymbol{H}_h^m\|^2 + 2\tau \sum_{n=1}^m \Big(R_e^{-1}\|\nabla\boldsymbol{u}_h^n\|^2 + \kappa R_m^{-1}\|\mathbf{curl}\,\boldsymbol{H}_h^n\|^2\Big) \le \|\boldsymbol{u}_h^0\|^2 + \kappa\|\boldsymbol{H}_h^0\|^2, \tag{25}$$

$$\kappa\|\mathbf{curl}\,\boldsymbol{A}_h^m\|^2 \le \|\boldsymbol{u}_h^0\|^2 + \kappa\|\boldsymbol{H}_h^0\|^2. \tag{26}$$

Proof. Taking $(\boldsymbol{v}_h, q_h, \boldsymbol{C}_h) = (\boldsymbol{u}_h^n, p_h^n, \kappa\boldsymbol{H}_h^n)$ in (19a)–(19c) and using the identity $2(a, a-b) = a^2 - b^2 + (a-b)^2$, we get

$$\frac{\|\boldsymbol{u}_h^n\|^2 - \|\boldsymbol{u}_h^{n-1}\|^2 + \|\boldsymbol{u}_h^n - \boldsymbol{u}_h^{n-1}\|^2}{2\tau} + R_e^{-1}\|\nabla\boldsymbol{u}_h^n\|^2 - \kappa(\mathbf{curl}\,\boldsymbol{H}_h^n \times \mathbf{curl}\,\boldsymbol{A}_h^n, \boldsymbol{u}_h^n) = 0,$$
$$\kappa\frac{\|\boldsymbol{H}_h^n\|^2 - \|\boldsymbol{H}_h^{n-1}\|^2 + \|\boldsymbol{H}_h^n - \boldsymbol{H}_h^{n-1}\|^2}{2\tau} + \kappa R_m^{-1}\|\mathbf{curl}\,\boldsymbol{H}_h^n\|^2 + \kappa(\mathbf{curl}\,\boldsymbol{A}_h^n \times \boldsymbol{u}_h^n, \mathbf{curl}\,\boldsymbol{H}_h^n) = 0.$$

Adding the resulting equations together, we obtain (23). Then we sum over the estimate (23) from 1 to m to get (25). Next, we take $(\boldsymbol{M}_h, \psi_h) = (\boldsymbol{A}_h^n, \phi_h^n)$ in (19d) and (19e) and using Cauchy–Schwarz inequality to get

$$\|\mathbf{curl}\,\boldsymbol{A}_h^n\|^2 = \big(\boldsymbol{H}_h^{n-1}, \mathbf{curl}\,\boldsymbol{A}_h^n\big) \le \|\boldsymbol{H}_h^{n-1}\|\|\mathbf{curl}\,\boldsymbol{A}_h^n\|,$$

which implies (24). To finish the proof, we combine (24) and (25) to obtain (26). $\qquad\square$

For the error estimates, we assume that the exact solution of MHD system (5) uniquely exists and the unknowns have following regularity property:

$$\begin{aligned}
&\boldsymbol{u} \in L^\infty\big(0, T; \boldsymbol{H}^{1+s}(\Omega)\big), \ \boldsymbol{u}_t \in L^2\big(0, T; \boldsymbol{H}^{1+s}(\Omega)\big), \ \boldsymbol{u}_{tt} \in L^2\big(0, T; \boldsymbol{H}^{-1}(\Omega)\big), \\
&p \in L^\infty(0, T; H^s(\Omega)), \ p_t \in L^2(0, T; H^s(\Omega)), \\
&\boldsymbol{H}, \mathbf{curl}\,\boldsymbol{H}, \boldsymbol{A}, \mathbf{curl}\,\boldsymbol{A} \in L^\infty(0, T; \boldsymbol{H}^s(\Omega)), \\
&\boldsymbol{H}_t, \mathbf{curl}\,\boldsymbol{H}_t \in L^2(0, T; \boldsymbol{H}^s(\Omega)), \ \boldsymbol{H}_{tt} \in L^2\big(0, T; (\boldsymbol{H}(\mathbf{curl}, \Omega))'\big),
\end{aligned} \tag{27}$$

where $s > \frac{1}{2}$. Under this assumption, our main error estimate result can be summarized as follows.

Theorem 4.3. *Let $(\boldsymbol{u}, p, \boldsymbol{H}, \boldsymbol{A}, \phi)$ be the exact solution of (5) with the regularity (27) holds. Let $(\boldsymbol{u}_h^n, p_h^n, \boldsymbol{H}_h^n, \boldsymbol{A}_h^n, \phi_h^n)$ be the numerical solution of the discrete system (19). Then we have the following error estimates for all $m = 1, 2, \cdots, N$,*

$$\|\boldsymbol{u}^m - \boldsymbol{u}_h^m\|^2 + \kappa\|\boldsymbol{H}^m - \boldsymbol{H}_h^m\|^2 + 2\tau \sum_{n=1}^m \Big(R_e^{-1}\|\nabla(\boldsymbol{u}^n - \boldsymbol{u}_h^n)\|^2 + \kappa R_m^{-1}\|\mathbf{curl}\,(\boldsymbol{H}^n - \boldsymbol{H}_h^n)\|^2\Big) \le C\big(h^{2\beta} + \tau^2\big), \tag{28}$$

$$\|\mathbf{curl}\,(\boldsymbol{A}^m - \boldsymbol{A}_h^m)\|^2 \le C\big(h^{2\beta} + \tau\big), \tag{29}$$

with $\beta = \min\{s, k\}$ and C is independent of the discrete parameters τ and h. If we further assume that $\boldsymbol{H}_t \in L^\infty(0, T; \boldsymbol{L}^2(\Omega))$, there holds that

$$\|\mathbf{curl}\,(\boldsymbol{A}^m - \boldsymbol{A}_h^m)\|^2 \le C(h^{2\beta} + \tau^2). \tag{30}$$

The detailed proof of this theorem will be given in Section 5.

Remark 4.4. In Theorem 4.3, the regularity assumption for the exact solutions is necessary to deliver the error estimates. Compared with the existing works [19, 42], the regularity for the exact solutions is relative weak and may be a reasonable hypothesis in such a setting of the general polyhedral domain with Lipschitz boundary. The interested readers can refer to [14] for regularity of classical MHD model and [6, 7] for Maxwell operator.

5. ERROR ANALYSIS

In this section, we carry out a rigorous error analysis for the proposed scheme.

5.1. Auxiliary estimates

In this subsection, we gather the necessary tools for the error estimates. First we present the classical and discrete Sobolev inequalities needed for the error estimates in the next subsection.

Lemma 5.1. *For $\boldsymbol{u} \in \boldsymbol{V}$, we have*

$$\|\boldsymbol{u}\|_{0,p} \leq C_p \|\nabla \boldsymbol{u}\|, \quad \text{for} \quad 1 \leq p \leq 6.$$

For $\boldsymbol{u} \in \boldsymbol{H}^{1+s}(\Omega)$ with $s > \frac{1}{2}$, we have

$$\|\boldsymbol{u}\|_{0,\infty} \leq C_\infty \|\boldsymbol{u}\|_{1+s}, \quad \|\nabla \boldsymbol{u}\|_{0,3} \leq C_e \|\boldsymbol{u}\|_{1+s}.$$

For $\boldsymbol{B} \in \boldsymbol{H}^s(\Omega)$ with $s > \frac{1}{2}$, we have

$$\|\boldsymbol{B}\|_{0,3} \leq C_m \|\boldsymbol{B}\|_s.$$

Next we define some projections of the unknowns and gather their approximation properties. For the fluid pair $(\boldsymbol{u}, p)$, we define the Stokes projection $(\mathcal{P}_h \boldsymbol{u}, \mathcal{Q}_h p) \in \boldsymbol{V}_h \times Q_h$ such that for all $(\boldsymbol{v}_h, q_h) \in \boldsymbol{V}_h \times Q_h$,

$$R_e^{-1}(\nabla \mathcal{P}_h \boldsymbol{u}, \nabla \boldsymbol{v}_h) - (\mathcal{Q}_h p, \nabla \cdot \boldsymbol{v}_h) = R_e^{-1}(\nabla \boldsymbol{u}, \nabla \boldsymbol{v}_h) - (p, \nabla \cdot \boldsymbol{v}_h), \tag{31a}$$

$$(\nabla \cdot \mathcal{P}_h \boldsymbol{u}, q_h) = (\nabla \cdot \boldsymbol{u}, q_h). \tag{31b}$$

For the magnetic field $\boldsymbol{H}$, we utilize the Fortin operator $\mathcal{F}_h : \boldsymbol{W} \to \boldsymbol{W}_h$, see [2, 43]. Given $\boldsymbol{H} \in \boldsymbol{W}$, we define $\mathcal{F}_h \boldsymbol{H} \in \boldsymbol{W}_h$ such that for all $(\boldsymbol{C}_h, s_h) \in \boldsymbol{W}_h \times R_h$,

$$(\mathbf{curl}\,(\mathcal{F}_h \boldsymbol{H}), \mathbf{curl}\,\boldsymbol{C}_h) = (\mathbf{curl}\,\boldsymbol{H}, \mathbf{curl}\,\boldsymbol{C}_h), \quad (\mathcal{F}_h \boldsymbol{H}, \nabla s_h) = (\boldsymbol{H}, \nabla s_h). \tag{32}$$

For the magnetic vector potential and Lagrange multiplier $(\boldsymbol{A}, \phi)$, we define the Maxwell projection $(\mathcal{R}_h \boldsymbol{A}, \mathcal{J}_h \phi) \in \boldsymbol{D}_h \times S_h$ such that for all $(\boldsymbol{M}_h, \psi_h) \in \boldsymbol{W}_h \times S_h$,

$$(\mathbf{curl}\,(\mathcal{R}_h \boldsymbol{A}), \mathbf{curl}\,\boldsymbol{M}_h) + (\nabla(\mathcal{J}_h \phi), \boldsymbol{M}_h) = (\mathbf{curl}\,\boldsymbol{A}, \mathbf{curl}\,\boldsymbol{M}_h) + (\nabla \phi, \boldsymbol{M}_h), \tag{33a}$$

$$(\mathcal{R}_h \boldsymbol{A}, \nabla \psi_h) = (\boldsymbol{A}, \nabla \psi_h). \tag{33b}$$

From [10, 15, 35, 36, 43], we have the following approximation property result for the projections.

Lemma 5.2. *Under the regularity assumption* (27), *the above projection satisfies*

$$\|\nabla(\boldsymbol{u} - \mathcal{P}_h \boldsymbol{u})\| + \|p - \mathcal{Q}_h p\| \leq Ch^\beta \big(\|\boldsymbol{u}\|_{1+s} + \|p\|_s\big),$$

$$\|\boldsymbol{u} - \mathcal{P}_h \boldsymbol{u}\| \leq Ch^{\beta + \min\{1,\beta\}} \big(\|\boldsymbol{u}\|_{1+s} + \|p\|_s\big),$$

$$\|\mathcal{P}_h \boldsymbol{u}\|_\infty + \|\nabla(\mathcal{P}_h \boldsymbol{u})\|_{0,3} \leq C_V \big(\|\boldsymbol{u}\|_{1+s} + \|p\|_s\big),$$

$$\|\boldsymbol{H} - \mathcal{F}_h \boldsymbol{H}\| + \|\mathbf{curl}\,(\boldsymbol{H} - \mathcal{F}_h \boldsymbol{H})\| \leq Ch^\beta(\|\boldsymbol{H}\|_s + \|\mathbf{curl}\,\boldsymbol{H}\|_s),$$

$$\|\mathbf{curl}\,(\mathcal{F}_h \boldsymbol{H})\|_{0,3} \leq C_W(\|\boldsymbol{H}\|_s + \|\mathbf{curl}\,\boldsymbol{H}\|_s),$$

$$\|\boldsymbol{A} - \mathcal{R}_h \boldsymbol{A}\| + \|\mathbf{curl}\,(\boldsymbol{A} - \mathcal{R}_h \boldsymbol{A})\| \leq Ch^\beta(\|\boldsymbol{A}\|_s + \|\mathbf{curl}\,\boldsymbol{A}\|_s).$$

with $\beta = \min\{s, k\}$.

As a consequence of the above result, we have that the initial errors satisfy

$$\left\|\boldsymbol{u}^0 - \boldsymbol{u}_h^0\right\| \leq Ch^{\beta+\min\{1,\beta\}}, \quad \left\|\nabla\left(\boldsymbol{u}^0 - \boldsymbol{u}_h^0\right)\right\| + \left\|\boldsymbol{H}^0 - \boldsymbol{H}_h^0\right\| \leq Ch^{\beta}. \tag{34}$$

Finally, we will frequently use the following discrete version of the Gronwall lemma [24].

Lemma 5.3. *Let* a_n, b_n, c_n *and* d_n *be non-negative numbers with* $n \geq 0$ *such that*

$$a_m + \tau \sum_{n=1}^{m} b_n \leq \tau \sum_{n=0}^{m-1} d_n a_n + \tau \sum_{n=0}^{m} c_n + C \qquad \forall m \geq 1,$$

where C *and* τ *are two positive constants. Then*

$$a_m + \tau \sum_{n=1}^{m} b_n \leq \exp\left(\tau \sum_{n=0}^{m-1} d_n\right)\left\{\tau \sum_{n=0}^{m} c_n + C\right\} \qquad \forall m \geq 1.$$

5.2. Error estimates

In this section, we derive error estimates for the fully discrete scheme of the MHD equations. In order to facilitate the subsequent error estimates, we define the following notations here and hereafter

$$e_\zeta = \zeta^n - \zeta_h^n = \theta_\zeta^n + \eta_\zeta^n, \quad \zeta = \boldsymbol{u}, p, \boldsymbol{H}, \boldsymbol{A}, \phi,$$

where the errors are decomposed into approximation errors θ_ζ^n and discretization errors η_ζ^n. The splittings are performed with the Stokes projection, the standard L^2-projection and the Fortin operator,

$$\theta_{\boldsymbol{u}} = \boldsymbol{u} - \mathcal{P}_h\boldsymbol{u}, \quad \theta_p = p - \mathcal{Q}_h p, \quad \theta_{\boldsymbol{H}} = \boldsymbol{H} - \mathcal{F}_h\boldsymbol{H}, \quad \theta_{\boldsymbol{A}} = \boldsymbol{A} - \mathcal{R}_h\boldsymbol{A}, \quad \theta_\phi = \phi - \mathcal{J}_h\phi,$$
$$\eta_{\boldsymbol{u}} = \mathcal{P}_h\boldsymbol{u} - \boldsymbol{u}_h, \quad \eta_p = \mathcal{Q}_h p - p_h, \quad \eta_{\boldsymbol{H}} = \mathcal{F}_h\boldsymbol{H} - \boldsymbol{H}_h, \quad \eta_{\boldsymbol{A}} = \mathcal{R}_h\boldsymbol{A} - \boldsymbol{A}_h, \quad \eta_\phi = \mathcal{J}_h\phi - \phi_h.$$

First we notice that the exact solutions of the system (5) satisfy the following variational equations at t_n for all $(\boldsymbol{v}_h, q_h, \boldsymbol{C}_h, \boldsymbol{M}_h, \psi_h) \in \boldsymbol{V}_h \times Q_h \times \boldsymbol{W}_h \times \boldsymbol{D}_h \times S_h$,

$$(\delta_t\boldsymbol{u}^n, \boldsymbol{v}_h) + R_e^{-1}(\nabla\boldsymbol{u}^n, \nabla\boldsymbol{v}_h)$$
$$+ \mathcal{O}\left(\boldsymbol{u}^{n-1}, \boldsymbol{u}^n, \boldsymbol{v}_h\right) - (p^n, \nabla\cdot\boldsymbol{v}_h) - \kappa(\mathbf{curl}\,\boldsymbol{H}^n \times \mathbf{curl}\,\boldsymbol{A}^n, \boldsymbol{v}_h) = (R_{\boldsymbol{u}}^n, \boldsymbol{v}_h), \tag{35a}$$
$$(\mathrm{div}\,\boldsymbol{u}^n, q_h) = 0, \tag{35b}$$
$$(\delta_t\boldsymbol{H}^n, \boldsymbol{C}_h) + R_m^{-1}(\mathbf{curl}\,\boldsymbol{H}^n, \mathbf{curl}\,\boldsymbol{C}_h) + (\mathbf{curl}\,\boldsymbol{A}^n \times \boldsymbol{u}^n, \mathbf{curl}\,\boldsymbol{C}_h) = (R_{\boldsymbol{H}}^n, \boldsymbol{C}_h), \tag{35c}$$
$$(\mathbf{curl}\,\boldsymbol{A}^n, \mathbf{curl}\,\boldsymbol{M}_h) + (\nabla\phi^n, \boldsymbol{M}_h) - \left(\boldsymbol{H}^{n-1}, \mathbf{curl}\,\boldsymbol{M}_h\right) = (R_{\boldsymbol{A}}^n, \boldsymbol{M}_h), \tag{35d}$$
$$(\boldsymbol{A}^n, \nabla\psi_h) = 0, \tag{35e}$$

where the truncation errors $R_{\boldsymbol{u}}^n, R_{\boldsymbol{H}}^n$ and $R_{\boldsymbol{A}}^n$ are defined by

$$(R_{\boldsymbol{u}}^n, \boldsymbol{v}_h) = (\delta_t\boldsymbol{u}^n - \boldsymbol{u}_t^n, \boldsymbol{v}_h) + \mathcal{O}\left(\boldsymbol{u}^{n-1} - \boldsymbol{u}^n, \boldsymbol{u}^n, \boldsymbol{v}_h\right),$$
$$(R_{\boldsymbol{H}}^n, \boldsymbol{C}_h) = (\delta_t\boldsymbol{H}^n - \boldsymbol{H}_t^n, \boldsymbol{C}_h),$$
$$(R_{\boldsymbol{A}}^n, \boldsymbol{M}_h) = \left(\boldsymbol{H}^n - \boldsymbol{H}^{n-1}, \mathbf{curl}\,\boldsymbol{M}_h\right).$$

In the following lemma, we estimate the residual terms $R_{\boldsymbol{u}}^n, R_{\boldsymbol{H}}^n$ and $R_{\boldsymbol{A}}^n$.

Lemma 5.4. *Suppose that* (27) *is satisfied, then we have*

$$\tau \sum_{n=1}^{N}\left(\|R_{\boldsymbol{u}}^n\|_{-1}^2 + \|R_{\boldsymbol{H}}^n\|_{(\boldsymbol{H}(\mathbf{curl},\Omega))'}^2 + \|R_{\boldsymbol{A}}^n\|_{(\boldsymbol{H}(\mathbf{curl},\Omega))'}^2\right) \leq C\tau^2.$$

Proof. From the definition of $R_{\boldsymbol{u}}^n$, using Hölder's inequality, Sobolev inequalities in Lemma 5.1 and (27), we arrive at

$$
\begin{aligned}
(R_{\boldsymbol{u}}^n, \boldsymbol{v}) &= \left(\frac{1}{\tau} \int_{t_{n-1}}^{t_n} (t_{n-1} - t) \boldsymbol{u}_{tt} \, \mathrm{d}t, \boldsymbol{v} \right) + \left(\left(\int_{t_n}^{t_{n-1}} \boldsymbol{u}_t \, \mathrm{d}t \right) \cdot \nabla \boldsymbol{u}^n, \boldsymbol{v} \right) \\
&\le \frac{1}{\tau} \left\| \int_{t_{n-1}}^{t_n} (t_{n-1} - t) \boldsymbol{u}_{tt} \, \mathrm{d}t \right\|_{\boldsymbol{H}^{-1}(\Omega)} \|\nabla \boldsymbol{v}\| + \left\| \int_{t_n}^{t_{n-1}} \boldsymbol{u}_t \, \mathrm{d}t \right\| \|\nabla \boldsymbol{u}^n\|_{0,3} \|\boldsymbol{v}\|_{0,6} \\
&\le C\sqrt{\tau} \|\boldsymbol{u}_{tt}\|_{L^2(t_{n-1}, t_n; \boldsymbol{H}^{-1}(\Omega))} \|\nabla \boldsymbol{v}\| + C\sqrt{\tau} \|\boldsymbol{u}_t\|_{L^2(t_{n-1}, t_n; \boldsymbol{L}^2(\Omega))} \|\boldsymbol{u}^n\|_{1+s} \|\nabla \boldsymbol{v}\|.
\end{aligned}
$$

Thus we have

$$
\|R_{\boldsymbol{u}}^n\|_{-1} \le \sup_{\boldsymbol{0} \ne \boldsymbol{v} \in \boldsymbol{V}} \frac{(R_{\boldsymbol{u}}^n, \boldsymbol{v})}{\|\nabla \boldsymbol{v}\|} \le C\sqrt{\tau} \Big(\|\boldsymbol{u}_{tt}\|_{L^2(t_{n-1}, t_n; \boldsymbol{H}^{-1}(\Omega))} + \|\boldsymbol{u}_t\|_{L^2(t_{n-1}, t_n; \boldsymbol{L}^2(\Omega))} \|\boldsymbol{u}^n\|_{1+s} \Big). \tag{36}
$$

Similarly,

$$
(R_{\boldsymbol{H}}^n, \boldsymbol{C}) = \left(\frac{1}{\tau} \int_{t_{n-1}}^{t_n} (t_{n-1} - t) \boldsymbol{H}_{tt} \, \mathrm{d}t, \boldsymbol{C} \right) \le C\sqrt{\tau} \|\boldsymbol{H}_{tt}\|_{L^2(t_{n-1}, t_n; (\boldsymbol{H}(\mathbf{curl}, \Omega))')} \|\mathbf{curl}\, \boldsymbol{C}\|,
$$

which means that

$$
\|R_{\boldsymbol{H}}^n\|_{(\boldsymbol{H}(\mathbf{curl}, \Omega))'} \le \sup_{\boldsymbol{0} \ne \boldsymbol{C} \in \boldsymbol{W}} \frac{(R_{\boldsymbol{H}}^n, \boldsymbol{C})}{\|\boldsymbol{C}\|_{\mathbf{curl}}} \le C\sqrt{\tau} \|\boldsymbol{H}_{tt}\|_{L^2(t_{n-1}, t_n; (\boldsymbol{H}(\mathbf{curl}, \Omega))')}.
$$

For the term $R_{\boldsymbol{A}}^n$, we estimate it as

$$
(R_{\boldsymbol{A}}^n, \boldsymbol{M}) = \left(\int_{t_{n-1}}^{t_n} \boldsymbol{H}_t \, \mathrm{d}t, \mathbf{curl}\, \boldsymbol{M} \right) \le C\sqrt{\tau} \|\boldsymbol{H}_t\|_{L^2(t_{n-1}, t_n; \boldsymbol{L}^2(\Omega))} \|\mathbf{curl}\, \boldsymbol{M}\|,
$$

which implies that

$$
\|R_{\boldsymbol{A}}^n\|_{(\boldsymbol{H}(\mathbf{curl}, \Omega))'} \le \sup_{\boldsymbol{0} \ne \boldsymbol{M} \in \boldsymbol{D}} \frac{(R_{\boldsymbol{A}}^n, \boldsymbol{M})}{\|\boldsymbol{M}\|_{\mathbf{curl}}} \le C\sqrt{\tau} \|\boldsymbol{H}_t\|_{L^2(t_{n-1}, t_n; \boldsymbol{L}^2(\Omega))}. \tag{37}
$$

This completes the proof. $\qquad\square$

Subtracting the numerical system (19) from the above system (35) and using the definitions of projections (31)–(33), we obtain the following error equations for all $(\boldsymbol{v}_h, q_h, \boldsymbol{C}_h, \boldsymbol{M}_h, \psi_h) \in \boldsymbol{V}_h \times Q_h \times \boldsymbol{W}_h \times \boldsymbol{D}_h \times S_h$,

$$
(\delta_t \eta_{\boldsymbol{u}}^n, \boldsymbol{v}_h) + R_e^{-1} (\nabla \eta_{\boldsymbol{u}}^n, \nabla \boldsymbol{v}_h) - (\eta_p^n, \nabla \cdot \boldsymbol{v}_h) = (R_{\boldsymbol{u}}^n, \boldsymbol{v}_h) - (\delta_t \theta_{\boldsymbol{u}}^n, \boldsymbol{v}_h) + \mathcal{C}(\boldsymbol{v}_h) + \mathcal{M}_1(\boldsymbol{v}_h), \tag{38a}
$$

$$
(\nabla \cdot \eta_{\boldsymbol{u}}^n, q_h) = 0, \tag{38b}
$$

$$
(\delta_t \eta_{\boldsymbol{H}}^n, \boldsymbol{C}_h) + R_m^{-1} (\mathbf{curl}\, \eta_{\boldsymbol{H}}^n, \mathbf{curl}\, \boldsymbol{C}_h) = (R_{\boldsymbol{H}}^n, \boldsymbol{C}_h) - (\delta_t \theta_{\boldsymbol{H}}^n, \boldsymbol{C}_h) + \mathcal{M}_2(\boldsymbol{C}_h), \tag{38c}
$$

$$
(\mathbf{curl}\, \eta_{\boldsymbol{A}}^n, \mathbf{curl}\, \boldsymbol{M}_h) + (\nabla \eta_\phi^n, \boldsymbol{M}_h) = (R_{\boldsymbol{A}}^n, \boldsymbol{M}_h) + \mathcal{M}_3(\boldsymbol{M}_h), \tag{38d}
$$

$$
(\eta_{\boldsymbol{A}}^n, \nabla \psi_h) = 0, \tag{38e}
$$

where the abbreviated terms are gathered as

$$
\begin{aligned}
\mathcal{C}(\boldsymbol{v}_h) &= \mathcal{O}(\boldsymbol{u}_h^{n-1}, \boldsymbol{u}_h^n, \boldsymbol{v}_h) - \mathcal{O}(\boldsymbol{u}^{n-1}, \boldsymbol{u}^n, \boldsymbol{v}_h), \\
\mathcal{M}_1(\boldsymbol{v}_h) &= \kappa(\mathbf{curl}\, \boldsymbol{H}^n \times \mathbf{curl}\, \boldsymbol{A}^n, \boldsymbol{v}_h) - \kappa(\mathbf{curl}\, \boldsymbol{H}_h^n \times \mathbf{curl}\, \boldsymbol{A}_h^n, \boldsymbol{v}_h), \\
\mathcal{M}_2(\boldsymbol{C}_h) &= (\mathbf{curl}\, \boldsymbol{A}_h^n \times \boldsymbol{u}_h^n, \mathbf{curl}\, \boldsymbol{C}_h) - (\mathbf{curl}\, \boldsymbol{A}^n \times \boldsymbol{u}^n, \mathbf{curl}\, \boldsymbol{C}_h), \\
\mathcal{M}_3(\boldsymbol{M}_h) &= (\boldsymbol{H}^{n-1} - \boldsymbol{H}_h^{n-1}, \mathbf{curl}\, \boldsymbol{M}_h).
\end{aligned}
$$

After the above preparation, we are now in a position to prove the error estimates.

Proof of Theorem 4.3. Taking $(\boldsymbol{v}_h, q_h, \boldsymbol{C}_h) = (\eta_{\boldsymbol{u}}^n, \eta_p^n, \kappa\eta_{\boldsymbol{H}}^n)$ in (38a)–(38c) and adding the three equations together, we obtain

$$
\frac{\|\eta_{\boldsymbol{u}}^n\|^2 - \|\eta_{\boldsymbol{u}}^{n-1}\|^2 + \|\eta_{\boldsymbol{u}}^n - \eta_{\boldsymbol{u}}^{n-1}\|^2}{2\tau} + \kappa\frac{\|\eta_{\boldsymbol{H}}^n\|^2 - \|\eta_{\boldsymbol{H}}^{n-1}\|^2 + \|\eta_{\boldsymbol{H}}^n - \eta_{\boldsymbol{H}}^{n-1}\|^2}{2\tau} + R_e^{-1}\|\nabla\eta_{\boldsymbol{u}}^n\|^2 + \kappa R_m^{-1}\|\mathbf{curl}\,\eta_{\boldsymbol{H}}^n\|^2
$$
$$
= (R_{\boldsymbol{u}}^n, \eta_{\boldsymbol{u}}^n) + \kappa(R_{\boldsymbol{H}}^n, \eta_{\boldsymbol{H}}^n) - (\delta_t\theta_{\boldsymbol{u}}^n, \eta_{\boldsymbol{u}}^n) - \kappa(\delta_t\theta_{\boldsymbol{H}}^n, \eta_{\boldsymbol{H}}^n) + \mathcal{C}(\eta_{\boldsymbol{u}}^n) + \mathcal{M}_1(\eta_{\boldsymbol{u}}^n) + \kappa\mathcal{M}_2(\eta_{\boldsymbol{H}}^n). \tag{39}
$$

We next bound the terms on the right hand side of the above identity one by one. For the first two terms on the right hand side of (39), using Cauchy–Schwarz inequality, Young inequality and (18), we have

$$
(R_{\boldsymbol{u}}^n, \eta_{\boldsymbol{u}}^n) \le \|R_{\boldsymbol{u}}^n\|_{-1}\|\nabla\eta_{\boldsymbol{u}}^n\| \le \frac{R_e^{-1}}{12}\|\nabla\eta_{\boldsymbol{u}}^n\|^2 + 3R_e\|R_{\boldsymbol{u}}^n\|_{-1}^2,
$$

$$
\kappa(R_{\boldsymbol{H}}^n, \eta_{\boldsymbol{H}}^n) \le \kappa C_*\|R_{\boldsymbol{H}}^n\|_{(\boldsymbol{H}(\mathbf{curl},\Omega))'}\|\mathbf{curl}\,\eta_{\boldsymbol{H}}^n\| \le \frac{\kappa R_m^{-1}}{8}\|\mathbf{curl}\,\eta_{\boldsymbol{H}}^n\|^2 + 2\kappa R_m C_*^2\|R_{\boldsymbol{H}}^n\|_{(\boldsymbol{H}(\mathbf{curl},\Omega))'}^2.
$$

Similarly, for the third and forth terms on the right hand side of (39), we get

$$
-(\delta_t\theta_{\boldsymbol{u}}^n, \eta_{\boldsymbol{u}}^n) \le \|\delta_t\theta_{\boldsymbol{u}}^n\|\|\eta_{\boldsymbol{u}}^n\| \le C_p\|\delta_t\theta_{\boldsymbol{u}}^n\|\|\nabla\eta_{\boldsymbol{u}}^n\| \le \frac{R_e^{-1}}{12}\|\nabla\eta_{\boldsymbol{u}}^n\|^2 + 3R_e C_p^2\|\delta_t\theta_{\boldsymbol{u}}^n\|^2,
$$

$$
-\kappa(\delta_t\theta_{\boldsymbol{H}}^n, \eta_{\boldsymbol{H}}^n) \le \kappa\|\delta_t\theta_{\boldsymbol{H}}^n\|\|\eta_{\boldsymbol{H}}^n\| \le \kappa C_*\|\delta_t\theta_{\boldsymbol{H}}^n\|\|\mathbf{curl}\,\eta_{\boldsymbol{H}}^n\| \le \frac{\kappa R_m^{-1}}{8}\|\mathbf{curl}\,\eta_{\boldsymbol{H}}^n\|^2 + 2\kappa R_m C_*^2\|\delta_t\theta_{\boldsymbol{H}}^n\|^2.
$$

For the fifth term, we rearrange it as follows,

$$
\begin{aligned}
\mathcal{C}(\eta_{\boldsymbol{u}}^n) &= \mathcal{O}(\boldsymbol{u}_h^{n-1}, \boldsymbol{u}_h^n, \eta_{\boldsymbol{u}}^n) - \mathcal{O}(\boldsymbol{u}^{n-1}, \boldsymbol{u}_h^n, \eta_{\boldsymbol{u}}^n) + \mathcal{O}(\boldsymbol{u}^{n-1}, \boldsymbol{u}_h^n, \eta_{\boldsymbol{u}}^n) - \mathcal{O}(\boldsymbol{u}^{n-1}, \boldsymbol{u}^n, \eta_{\boldsymbol{u}}^n) \\
&= -\mathcal{O}(e_{\boldsymbol{u}}^{n-1}, \boldsymbol{u}_h^n, \eta_{\boldsymbol{u}}^n) - \mathcal{O}(\boldsymbol{u}^{n-1}, e_{\boldsymbol{u}}^n, \eta_{\boldsymbol{u}}^n) \\
&= -\mathcal{O}(\theta_{\boldsymbol{u}}^{n-1}, \mathcal{P}_h\boldsymbol{u}^n, \eta_{\boldsymbol{u}}^n) - \mathcal{O}(\eta_{\boldsymbol{u}}^{n-1}, \mathcal{P}_h\boldsymbol{u}^n, \eta_{\boldsymbol{u}}^n) - \mathcal{O}(\boldsymbol{u}^{n-1}, \theta_{\boldsymbol{u}}^n, \eta_{\boldsymbol{u}}^n).
\end{aligned}
$$

The terms in the last step can be bounded using Hölder's inequality, Sobolev inequalities in Lemma 5.1 and the approximation properties of the projections in Lemma 5.2 as,

$$
\begin{aligned}
-\mathcal{O}(\theta_{\boldsymbol{u}}^{n-1}, \mathcal{P}_h\boldsymbol{u}^n, \eta_{\boldsymbol{u}}^n) &\le \frac{1}{2}\|\theta_{\boldsymbol{u}}^{n-1}\|\|\nabla(\mathcal{P}_h\boldsymbol{u}^n)\|_{0,3}\|\eta_{\boldsymbol{u}}^n\|_{0,6} + \frac{1}{2}\|\theta_{\boldsymbol{u}}^{n-1}\|\|\nabla\eta_{\boldsymbol{u}}^n\|\|\mathcal{P}_h\boldsymbol{u}^n\|_{0,\infty} \\
&\le \frac{1}{2}(C_p+1)C_V\|\theta_{\boldsymbol{u}}^{n-1}\|(\|\boldsymbol{u}^n\|_{1+s} + \|p^n\|_s)\|\nabla\eta_{\boldsymbol{u}}^n\| \\
&\le \frac{R_e^{-1}}{18}\|\nabla\eta_{\boldsymbol{u}}^n\|^2 + \frac{9R_e}{4}(C_p+1)^2 C_V^2\|\theta_{\boldsymbol{u}}^{n-1}\|^2\left(\|\boldsymbol{u}^n\|_{1+s}^2 + \|p^n\|_s^2\right), \\
-\mathcal{O}(\eta_{\boldsymbol{u}}^{n-1}, \mathcal{P}_h\boldsymbol{u}^n, \eta_{\boldsymbol{u}}^n) &\le \frac{1}{2}\|\eta_{\boldsymbol{u}}^{n-1}\|\|\mathcal{P}_h\boldsymbol{u}^n\|_{0,3}\|\eta_{\boldsymbol{u}}^n\|_{0,6} + \frac{1}{2}\|\eta_{\boldsymbol{u}}^{n-1}\|\|\mathcal{P}_h\boldsymbol{u}^n\|_{0,\infty}\|\nabla\eta_{\boldsymbol{u}}^n\| \\
&\le \frac{1}{2}(C_p+1)C_V\|\eta_{\boldsymbol{u}}^{n-1}\|(\|\boldsymbol{u}^n\|_{1+s} + \|p^n\|_s)\|\nabla\eta_{\boldsymbol{u}}^n\| \\
&\le \frac{R_e^{-1}}{18}\|\nabla\eta_{\boldsymbol{u}}^n\|^2 + \frac{9R_e}{4}(C_p+1)^2 C_V^2\|\eta_{\boldsymbol{u}}^{n-1}\|^2\left(\|\boldsymbol{u}^n\|_{1+s}^2 + \|p^n\|_s^2\right), \\
-\mathcal{O}(\boldsymbol{u}^{n-1}, \theta_{\boldsymbol{u}}^n, \eta_{\boldsymbol{u}}^n) &\le \|\boldsymbol{u}^{n-1}\|_{0,3}\|\nabla\theta_{\boldsymbol{u}}^n\|\|\eta_{\boldsymbol{u}}^n\|_{0,6} \le C_p^2\|\nabla\boldsymbol{u}^{n-1}\|\|\nabla\theta_{\boldsymbol{u}}^n\|\|\nabla\eta_{\boldsymbol{u}}^n\| \\
&\le \frac{R_e^{-1}}{18}\|\nabla\eta_{\boldsymbol{u}}^n\|^2 + \frac{9R_e}{2}C_p^4\|\nabla\boldsymbol{u}^{n-1}\|^2\|\nabla\theta_{\boldsymbol{u}}^n\|^2.
\end{aligned}
$$

Thus, we conclude that

$$
\mathcal{C}(\eta_{\boldsymbol{u}}^n) \le \frac{R_e^{-1}}{6}\|\nabla\eta_{\boldsymbol{u}}^n\|^2 + \frac{9R_e}{4}(C_p+1)^2 C_V^2\|\theta_{\boldsymbol{u}}^{n-1}\|^2\left(\|\boldsymbol{u}^n\|_{1+s}^2 + \|p^n\|_s^2\right)
$$

$$+ \frac{9R_e}{4}(C_p+1)^2 C_V^2 \big\|\eta_{\boldsymbol{u}}^{n-1}\big\|^2 \Big(\|\boldsymbol{u}^n\|_{1+s}^2 + \|p^n\|_s^2\Big) + \frac{9R_e}{2}C_p^4 \big\|\nabla\boldsymbol{u}^{n-1}\big\|^2 \|\nabla\theta_{\boldsymbol{u}}^n\|^2. \tag{40}$$

For the last two terms on the right hand side of (39), we rearrange them as follows:

$$\mathcal{M}_1(\eta_{\boldsymbol{u}}^n) + \kappa\mathcal{M}_2(\eta_{\boldsymbol{H}}^n) = \kappa(\mathbf{curl}\,(\boldsymbol{H}^n - \boldsymbol{H}_h^n) \times \mathbf{curl}\,\boldsymbol{A}^n, \eta_{\boldsymbol{u}}^n) + \kappa(\mathbf{curl}\,\boldsymbol{H}_h^n \times \mathbf{curl}\,(\boldsymbol{A}^n - \boldsymbol{A}_h^n), \eta_{\boldsymbol{u}}^n)$$
$$+ \kappa((\boldsymbol{u}^n - \boldsymbol{u}_h^n) \times \mathbf{curl}\,\boldsymbol{A}^n, \mathbf{curl}\,\eta_{\boldsymbol{H}}^n) + \kappa(\boldsymbol{u}_h^n \times \mathbf{curl}\,(\boldsymbol{A}^n - \boldsymbol{A}_h^n), \mathbf{curl}\,\eta_{\boldsymbol{H}}^n)$$
$$= M_1 + M_2 + M_3 + M_4.$$

Next we will estimate $M_1 + M_3$ and $M_2 + M_4$ separately. For the terms $M_1 + M_3$, we have

$$M_1 + M_3 = \kappa(\mathbf{curl}\,(\theta_{\boldsymbol{H}}^n + \eta_{\boldsymbol{H}}^n) \times \mathbf{curl}\,\boldsymbol{A}^n, \eta_{\boldsymbol{u}}^n) + \kappa((\theta_{\boldsymbol{u}}^n + \eta_{\boldsymbol{u}}^n) \times \mathbf{curl}\,\boldsymbol{A}^n, \mathbf{curl}\,\eta_{\boldsymbol{H}}^n)$$
$$= \kappa(\mathbf{curl}\,\theta_{\boldsymbol{H}}^n \times \mathbf{curl}\,\boldsymbol{A}^n, \eta_{\boldsymbol{u}}^n) + \kappa(\theta_{\boldsymbol{u}}^n \times \mathbf{curl}\,\boldsymbol{A}^n, \mathbf{curl}\,\eta_{\boldsymbol{H}}^n)$$
$$+ \kappa(\mathbf{curl}\,\eta_{\boldsymbol{H}}^n \times \mathbf{curl}\,\boldsymbol{A}^n, \eta_{\boldsymbol{u}}^n) + \kappa(\eta_{\boldsymbol{u}}^n \times \mathbf{curl}\,\boldsymbol{A}^n, \mathbf{curl}\,\eta_{\boldsymbol{H}}^n)$$
$$= \kappa(\mathbf{curl}\,\theta_{\boldsymbol{H}}^n \times \mathbf{curl}\,\boldsymbol{A}^n, \eta_{\boldsymbol{u}}^n) + \kappa(\theta_{\boldsymbol{u}}^n \times \mathbf{curl}\,\boldsymbol{A}^n, \mathbf{curl}\,\eta_{\boldsymbol{H}}^n),$$

where we have used the fact $(\boldsymbol{a}\times\boldsymbol{b}, \boldsymbol{c}) + (\boldsymbol{c}\times\boldsymbol{b}, \boldsymbol{a}) = 0$ to cancel the last two terms out in last equality. Using Hölder's inequality and Young's inequality, we get

$$M_1 + M_3 = \kappa(\mathbf{curl}\,\theta_{\boldsymbol{H}}^n \times \mathbf{curl}\,\boldsymbol{A}^n, \eta_{\boldsymbol{u}}^n) + \kappa(\theta_{\boldsymbol{u}}^n \times \mathbf{curl}\,\boldsymbol{A}^n, \mathbf{curl}\,\eta_{\boldsymbol{H}}^n)$$
$$\leq \kappa\|\mathbf{curl}\,\theta_{\boldsymbol{H}}^n\|\|\mathbf{curl}\,\boldsymbol{A}^n\|_{0,3}\|\eta_{\boldsymbol{u}}^n\|_{0,6} + \kappa\|\theta_{\boldsymbol{u}}^n\|_{0,6}\|\mathbf{curl}\,\boldsymbol{A}^n\|_{0,3}\|\mathbf{curl}\,\eta_{\boldsymbol{H}}^n\|$$
$$\leq C_p\kappa C_m\|\mathbf{curl}\,\theta_{\boldsymbol{H}}^n\|\|\mathbf{curl}\,\boldsymbol{A}^n\|_s\|\nabla\eta_{\boldsymbol{u}}^n\| + C_p\kappa C_m\|\nabla\theta_{\boldsymbol{u}}^n\|\|\mathbf{curl}\,\boldsymbol{A}^n\|_s\|\mathbf{curl}\,\eta_{\boldsymbol{H}}^n\|$$
$$\leq \frac{R_e^{-1}}{12}\|\nabla\eta_{\boldsymbol{u}}^n\|^2 + \frac{\kappa R_m^{-1}}{8}\|\mathbf{curl}\,\eta_{\boldsymbol{H}}^n\|^2 + 3R_e C_p^2\kappa^2 C_m^2\|\mathbf{curl}\,\theta_{\boldsymbol{H}}^n\|^2\|\mathbf{curl}\,\boldsymbol{A}^n\|_s^2$$
$$+ 2R_m C_p^2\kappa C_m^2\|\nabla\theta_{\boldsymbol{u}}^n\|^2\|\mathbf{curl}\,\boldsymbol{A}^n\|_s^2.$$

For the terms $M_2 + M_4$, we insert the following identity into them,

$$\kappa(\mathbf{curl}\,\eta_{\boldsymbol{H}}^n \times \mathbf{curl}\,(\boldsymbol{A}^n - \boldsymbol{A}_h^n), \eta_{\boldsymbol{u}}^n) + \kappa(\eta_{\boldsymbol{u}}^n \times \mathbf{curl}\,(\boldsymbol{A}^n - \boldsymbol{A}_h^n), \mathbf{curl}\,\eta_{\boldsymbol{H}}^n) = 0,$$

to get

$$M_2 + M_4 = \kappa(\mathbf{curl}\,(\mathcal{F}_h\boldsymbol{H}^n) \times \mathbf{curl}\,(\boldsymbol{A}^n - \boldsymbol{A}_h^n), \eta_{\boldsymbol{u}}^n) + \kappa(\mathcal{P}_h\boldsymbol{u}^n \times \mathbf{curl}\,(\boldsymbol{A}^n - \boldsymbol{A}_h^n), \mathbf{curl}\,\eta_{\boldsymbol{H}}^n)$$
$$= \kappa(\mathbf{curl}\,(\mathcal{F}_h\boldsymbol{H}^n) \times \mathbf{curl}\,\theta_{\boldsymbol{A}}^n, \eta_{\boldsymbol{u}}^n) + \kappa(\mathcal{P}_h\boldsymbol{u}^n \times \mathbf{curl}\,\theta_{\boldsymbol{A}}^n, \mathbf{curl}\,\eta_{\boldsymbol{H}}^n)$$
$$+ \kappa(\mathbf{curl}\,(\mathcal{F}_h\boldsymbol{H}^n) \times \mathbf{curl}\,\eta_{\boldsymbol{A}}^n, \eta_{\boldsymbol{u}}^n) + \kappa(\mathcal{P}_h\boldsymbol{u}^n \times \mathbf{curl}\,\eta_{\boldsymbol{A}}^n, \mathbf{curl}\,\eta_{\boldsymbol{H}}^n).$$

Applying Hölder's inequality, Young's inequality and the stability of the projections in Lemma 5.2, we have

$$M_2 + M_4 \leq \kappa\|\mathbf{curl}\,(\mathcal{F}_h\boldsymbol{H}^n)\|_{0,3}\|\mathbf{curl}\,\theta_{\boldsymbol{A}}^n\|\|\eta_{\boldsymbol{u}}^n\|_{0,6} + \kappa\|\mathbf{curl}\,(\mathcal{F}_h\boldsymbol{H}^n)\|_{0,3}\|\mathbf{curl}\,\eta_{\boldsymbol{A}}^n\|\|\eta_{\boldsymbol{u}}^n\|_{0,6}$$
$$+ \kappa\|\mathcal{P}_h\boldsymbol{u}^n\|_{0,\infty}\|\mathbf{curl}\,\theta_{\boldsymbol{A}}^n\|\|\mathbf{curl}\,\eta_{\boldsymbol{H}}^n\| + \kappa\|\mathcal{P}_h\boldsymbol{u}^n\|_{0,\infty}\|\mathbf{curl}\,\eta_{\boldsymbol{A}}^n\|\|\mathbf{curl}\,\eta_{\boldsymbol{H}}^n\|$$
$$\leq C_W C_p\kappa(\|\boldsymbol{H}^n\|_s + \|\mathbf{curl}\,\boldsymbol{H}^n\|_s)\|\mathbf{curl}\,\theta_{\boldsymbol{A}}^n\|\|\nabla\eta_{\boldsymbol{u}}^n\| + C_W C_p\kappa(\|\boldsymbol{H}^n\|_s + \|\mathbf{curl}\,\boldsymbol{H}^n\|_s)\|\mathbf{curl}\,\eta_{\boldsymbol{A}}^n\|\|\nabla\eta_{\boldsymbol{u}}^n\|$$
$$+ C_V\kappa(\|\boldsymbol{u}^n\|_{1+s} + \|p^n\|_s)\|\mathbf{curl}\,\theta_{\boldsymbol{A}}^n\|\|\mathbf{curl}\,\eta_{\boldsymbol{H}}^n\| + C_V\kappa(\|\boldsymbol{u}^n\|_{1+s} + \|p^n\|_s)\|\mathbf{curl}\,\eta_{\boldsymbol{A}}^n\|\|\mathbf{curl}\,\eta_{\boldsymbol{H}}^n\|$$
$$\leq \frac{R_e^{-1}}{12}\|\nabla\eta_{\boldsymbol{u}}^n\|^2 + \frac{\kappa R_m^{-1}}{8}\|\mathbf{curl}\,\eta_{\boldsymbol{H}}^n\|^2 + 12R_e C_W^2 C_p^2\kappa^2\Big(\|\boldsymbol{H}^n\|_s^2 + \|\mathbf{curl}\,\boldsymbol{H}^n\|_s^2\Big)\|\mathbf{curl}\,\theta_{\boldsymbol{A}}^n\|^2$$
$$+ 12R_e C_W^2 C_p^2\kappa^2\Big(\|\boldsymbol{H}^n\|_s^2 + \|\mathbf{curl}\,\boldsymbol{H}^n\|_s^2\Big)\|\mathbf{curl}\,\eta_{\boldsymbol{A}}^n\|^2 + 8R_m C_V^2\kappa\Big(\|\boldsymbol{u}^n\|_{1+s}^2 + \|p^n\|_s^2\Big)\|\mathbf{curl}\,\theta_{\boldsymbol{A}}^n\|^2$$
$$+ 8R_m C_V^2\kappa\Big(\|\boldsymbol{u}^n\|_{1+s}^2 + \|p^n\|_s^2\Big)\|\mathbf{curl}\,\eta_{\boldsymbol{A}}^n\|^2. \tag{41}$$

To deal with the term $\|\mathbf{curl}\,\eta_{\boldsymbol{A}}^n\|$ on the right hand side of (41), we take $(\boldsymbol{M}_h, \psi_h) = (\eta_{\boldsymbol{A}}^n, \eta_\phi^n)$ in (38d) and (38e) to get

$$\|\mathbf{curl}\,\eta_{\boldsymbol{A}}^n\|^2 = (R_{\boldsymbol{A}}^n, \eta_{\boldsymbol{A}}^n) + \mathcal{M}_3(\eta_{\boldsymbol{A}}^n) = (R_{\boldsymbol{A}}^n, \eta_{\boldsymbol{A}}^n) + \left(\eta_{\boldsymbol{H}}^{n-1} + \theta_{\boldsymbol{H}}^{n-1}, \mathbf{curl}\,\eta_{\boldsymbol{A}}^n\right)$$
$$\leq C_* \|R_{\boldsymbol{A}}^n\|_{(\boldsymbol{H}(\mathbf{curl},\Omega))'}\|\mathbf{curl}\,\eta_{\boldsymbol{A}}^n\| + \|\eta_{\boldsymbol{H}}^{n-1}\|\|\mathbf{curl}\,\eta_{\boldsymbol{A}}^n\| + \|\theta_{\boldsymbol{H}}^{n-1}\|\|\mathbf{curl}\,\eta_{\boldsymbol{A}}^n\|,$$

which means that

$$\|\mathbf{curl}\,\eta_{\boldsymbol{A}}^n\|^2 \leq 3C_*^2 \|R_{\boldsymbol{A}}^n\|_{(\boldsymbol{H}(\mathbf{curl},\Omega))'}^2 + 3\|\eta_{\boldsymbol{H}}^{n-1}\|^2 + 3\|\theta_{\boldsymbol{H}}^{n-1}\|^2. \tag{42}$$

Thus, we have

$$M_2 + M_4 \leq \frac{R_e^{-1}}{12}\|\nabla\eta_{\boldsymbol{u}}^n\|^2 + \frac{\kappa R_m^{-1}}{8}\|\mathbf{curl}\,\eta_{\boldsymbol{H}}^n\|^2 + 12R_e C_W^2 C_p^2 \kappa^2 \left(\|\boldsymbol{H}^n\|_s^2 + \|\mathbf{curl}\,\boldsymbol{H}^n\|_s^2\right)\|\mathbf{curl}\,\theta_{\boldsymbol{A}}^n\|^2$$
$$+ 36R_e C_W^2 C_p^2 \kappa^2 \left(\|\boldsymbol{H}^n\|_s^2 + \|\mathbf{curl}\,\boldsymbol{H}^n\|_s^2\right)\left(C_*^2\|R_{\boldsymbol{A}}^n\|_{(\boldsymbol{H}(\mathbf{curl},\Omega))'}^2 + \|\eta_{\boldsymbol{H}}^{n-1}\|^2 + \|\theta_{\boldsymbol{H}}^{n-1}\|^2\right)$$
$$+ 8R_m C_V^2 \kappa\left(\|\boldsymbol{u}^n\|_{1+s}^2 + \|p^n\|_s^2\right)\|\mathbf{curl}\,\theta_{\boldsymbol{A}}^n\|^2$$
$$+ 24R_m C_V^2 \kappa\left(\|\boldsymbol{u}^n\|_{1+s}^2 + \|p^n\|_s^2\right)\left(C_*^2\|R_{\boldsymbol{A}}^n\|_{(\boldsymbol{H}(\mathbf{curl},\Omega))'}^2 + \|\eta_{\boldsymbol{H}}^{n-1}\|^2 + \|\theta_{\boldsymbol{H}}^{n-1}\|^2\right). \tag{43}$$

Hence, we derive that

$$\mathcal{M}_1(\eta_{\boldsymbol{u}}^n) + \kappa\mathcal{M}_2(\eta_{\boldsymbol{H}}^n) \leq \frac{R_e^{-1}}{6}\|\nabla\eta_{\boldsymbol{u}}^n\|^2 + \frac{\kappa R_m^{-1}}{4}\|\mathbf{curl}\,\eta_{\boldsymbol{H}}^n\|^2 + 3R_e C_p^2 \kappa^2 C_m^2 \|\mathbf{curl}\,\theta_{\boldsymbol{H}}^n\|^2\|\mathbf{curl}\,\boldsymbol{A}^n\|_s^2$$
$$+ 2R_m C_p^2 \kappa C_m^2 \|\nabla\theta_{\boldsymbol{u}}^n\|^2\|\mathbf{curl}\,\boldsymbol{A}^n\|_s^2 + 12C_W^2 C_p^2 \kappa^2 \left(\|\boldsymbol{H}^n\|_s^2 + \|\mathbf{curl}\,\boldsymbol{H}^n\|_s^2\right)\|\mathbf{curl}\,\theta_{\boldsymbol{A}}^n\|^2$$
$$+ 36R_e C_W^2 C_p^2 \kappa^2 \left(\|\boldsymbol{H}^n\|_s^2 + \|\mathbf{curl}\,\boldsymbol{H}^n\|_s^2\right)\left(C_*^2\|R_{\boldsymbol{A}}^n\|_{(\boldsymbol{H}(\mathbf{curl},\Omega))'}^2 + \|\eta_{\boldsymbol{H}}^{n-1}\|^2 + \|\theta_{\boldsymbol{H}}^{n-1}\|^2\right)$$
$$+ 8R_m C_V^2 \kappa\left(\|\boldsymbol{u}^n\|_{1+s}^2 + \|p^n\|_s^2\right)\|\mathbf{curl}\,\theta_{\boldsymbol{A}}^n\|^2$$
$$+ 24R_m C_V^2 \kappa\left(\|\boldsymbol{u}^n\|_{1+s}^2 + \|p^n\|_s^2\right)\left(C_*^2\|R_{\boldsymbol{A}}^n\|_{(\boldsymbol{H}(\mathbf{curl},\Omega))'}^2 + \|\eta_{\boldsymbol{H}}^{n-1}\|^2 + \|\theta_{\boldsymbol{H}}^{n-1}\|^2\right). \tag{44}$$

Combining all the above estimates, we arrive at

$$\frac{\|\eta_{\boldsymbol{u}}^n\|^2 - \|\eta_{\boldsymbol{u}}^{n-1}\|^2 + \|\eta_{\boldsymbol{u}}^n - \eta_{\boldsymbol{u}}^{n-1}\|^2}{2\tau} + \kappa\frac{\|\eta_{\boldsymbol{H}}^n\|^2 - \|\eta_{\boldsymbol{H}}^{n-1}\|^2 + \|\eta_{\boldsymbol{H}}^n - \eta_{\boldsymbol{H}}^{n-1}\|^2}{2\tau}$$
$$+ \frac{R_e^{-1}}{2}\|\nabla\eta_{\boldsymbol{u}}^n\|^2 + \frac{\kappa R_m^{-1}}{2}\|\mathbf{curl}\,\eta_{\boldsymbol{H}}^n\|^2$$
$$\leq \frac{9R_e}{4}(C_p + 1)^2 C_V^2 \left(\|\boldsymbol{u}^n\|_{1+s}^2 + \|p^n\|_s^2\right)\|\eta_{\boldsymbol{u}}^{n-1}\|^2$$
$$+ \left(36R_e C_W^2 C_p^2 \kappa^2 \left(\|\boldsymbol{H}^n\|_s^2 + \|\mathbf{curl}\,\boldsymbol{H}^n\|_s^2\right) + 24R_m C_V^2 \kappa\left(\|\boldsymbol{u}^n\|_{1+s}^2 + \|p^n\|_s^2\right)\right)\|\eta_{\boldsymbol{H}}^{n-1}\|^2$$
$$+ 3R_e \|R_{\boldsymbol{u}}^n\|_{-1}^2 + 2\kappa R_m C_*^2 \|R_{\boldsymbol{H}}^n\|_{(\boldsymbol{H}(\mathbf{curl},\Omega))'}^2 + 3R_e C_p^2 \|\delta_t\theta_{\boldsymbol{u}}^n\|^2 + 2\kappa R_m C_*^2 \|\delta_t\theta_{\boldsymbol{H}}^n\|^2$$
$$+ \frac{9R_e}{2}C_p^4 \|\nabla\boldsymbol{u}^{n-1}\|^2\|\nabla\theta_{\boldsymbol{u}}^n\|^2 + \frac{9R_e}{4}(C_p + 1)^2 C_V^2 \|\theta_{\boldsymbol{u}}^{n-1}\|^2\left(\|\boldsymbol{u}^n\|_{1+s}^2 + \|p^n\|_s^2\right)$$
$$+ 3R_e C_p^2 \kappa^2 C_m^2 \|\mathbf{curl}\,\theta_{\boldsymbol{H}}^n\|^2\|\mathbf{curl}\,\boldsymbol{A}^n\|_s^2 + 2R_m C_p^2 \kappa C_m^2 \|\nabla\theta_{\boldsymbol{u}}^n\|^2\|\mathbf{curl}\,\boldsymbol{A}^n\|_s^2$$
$$+ 12R_e C_W^2 C_p^2 \kappa^2 \left(\|\boldsymbol{H}^n\|_s^2 + \|\mathbf{curl}\,\boldsymbol{H}^n\|_s^2\right)\|\mathbf{curl}\,\theta_{\boldsymbol{A}}^n\|^2 + 8R_m C_V^2 \kappa\left(\|\boldsymbol{u}^n\|_{1+s}^2 + \|p^n\|_s^2\right)\|\mathbf{curl}\,\theta_{\boldsymbol{A}}^n\|^2$$
$$+ 36R_e C_W^2 C_p^2 \kappa^2 \left(\|\boldsymbol{H}^n\|_s^2 + \|\mathbf{curl}\,\boldsymbol{H}^n\|_s^2\right)\left(C_*^2\|R_{\boldsymbol{A}}^n\|_{(\boldsymbol{H}(\mathbf{curl},\Omega))'}^2 + \|\theta_{\boldsymbol{H}}^{n-1}\|^2\right)$$
$$+ 24R_m C_V^2 \kappa\left(\|\boldsymbol{u}^n\|_{1+s}^2 + \|p^n\|_s^2\right)\left(C_*^2\|R_{\boldsymbol{A}}^n\|_{(\boldsymbol{H}(\mathbf{curl},\Omega))'}^2 + \|\theta_{\boldsymbol{H}}^{n-1}\|^2\right). \tag{45}$$

Before proceeding with the analysis, we notice that the following estimates hold

$$\tau \sum_{n=1}^{m} \|\delta_t \theta_{\boldsymbol{u}}^n\|^2 \leq C h^{2\beta} \Big(\|\boldsymbol{u}_t\|_{L^2(0,t_m;\boldsymbol{H}^{1+s})}^2 + \|p_t\|_{L^2(0,t_m;H^s)}^2 \Big),$$

$$\tau \sum_{n=1}^{m} \|\delta_t \theta_{\boldsymbol{H}}^n\|^2 \leq C h^{2\beta} \Big(\|\boldsymbol{H}_t\|_{L^2(0,t_m;\boldsymbol{H}^s(\Omega))}^2 + \|\mathbf{curl}\, \boldsymbol{H}_t\|_{L^2(0,t_m;\boldsymbol{H}^s(\Omega))}^2 \Big).$$

Multiplying 2τ on the estimate (45), summing over $n = 1, \cdots, m$, using the fact $\eta_{\boldsymbol{u}}^0 = \eta_{\boldsymbol{H}}^0 = \boldsymbol{0}$, the regularity assumption (27) and the approximation properties of the projections in Lemma 5.2, we have

$$\|\eta_{\boldsymbol{u}}^m\|^2 + \kappa \|\eta_{\boldsymbol{H}}^m\|^2 + \tau \sum_{n=1}^{m} \Big(R_e^{-1} \|\nabla \eta_{\boldsymbol{u}}^n\|^2 + \kappa R_m^{-1} \|\mathbf{curl}\, \eta_{\boldsymbol{H}}^n\|^2 \Big) \leq \tau \hat{C} \sum_{n=1}^{m} \Big(\|\eta_{\boldsymbol{u}}^{n-1}\|^2 + \|\eta_{\boldsymbol{H}}^{n-1}\|^2 \Big)$$
$$+ C\tau^2 + C h^{2\beta}, \tag{46}$$

where $\hat{C}$ is given by

$$\hat{C} = \frac{9R_e}{2}(C_p + 1)^2 C_V^2 \Big(\|\boldsymbol{u}\|_{L^\infty(0,t_m;\boldsymbol{H}^{1+s}(\Omega))}^2 + \|p\|_{L^\infty(0,t_m;H^s(\Omega))}^2 \Big)$$
$$+ 72 R_e C_W^2 C_p^2 \kappa^2 \Big(\|\boldsymbol{H}\|_{L^\infty(0,t_m;\boldsymbol{H}^s(\Omega))}^2 + \|\mathbf{curl}\, \boldsymbol{H}\|_{L^\infty(0,t_m;\boldsymbol{H}^s(\Omega))}^2 \Big)$$
$$+ 48 R_m C_V^2 \kappa \Big(\|\boldsymbol{u}\|_{L^\infty(0,t_m;\boldsymbol{H}^{1+s}(\Omega))}^2 + \|p\|_{L^\infty(0,t_m;H^s(\Omega))}^2 \Big). \tag{47}$$

By the discrete Gronwall inequality, we have

$$\|\eta_{\boldsymbol{u}}^m\|^2 + \kappa \|\eta_{\boldsymbol{H}}^m\|^2 + \tau \sum_{n=1}^{m} \Big(R_e^{-1} \|\nabla \eta_{\boldsymbol{u}}^n\|^2 + \kappa R_m^{-1} \|\mathbf{curl}\, \eta_{\boldsymbol{H}}^n\|^2 \Big) \leq C(h^{2\beta} + \tau^2). \tag{48}$$

We complete the proof of the error estimates for $\boldsymbol{u}$ and $\boldsymbol{H}$ in (28) by applying the triangle inequality, the approximation properties of the projections in Lemma 5.2 together with above estimates.

With the above estimates for $\boldsymbol{u}$ and $\boldsymbol{H}$, we invoke with (42) and the approximation properties of the projections in Lemma 5.2 to get

$$\|\mathbf{curl}\, \eta_{\boldsymbol{A}}^n\|^2 \leq 3\|R_{\boldsymbol{A}}^n\|_{(\boldsymbol{H}(\mathbf{curl},\Omega))'}^2 + C(h^{2\beta} + \tau^2). \tag{49}$$

Using (37) with the triangle inequality, we obtain the error estimate (29) for $\boldsymbol{A}$.

With a slightly stronger regularity assumption with $\boldsymbol{H}_t \in L^\infty(0,T;\boldsymbol{L}^2(\Omega))$, we have

$$(R_{\boldsymbol{A}}^n, \boldsymbol{M}) = \left(\int_{t_{n-1}}^{t_n} \boldsymbol{H}_t \, \mathrm{d}t, \mathbf{curl}\, \boldsymbol{M} \right) \leq C\tau \|\boldsymbol{H}_t\|_{L^\infty(t_{n-1},t_n;\boldsymbol{L}^2(\Omega))} \|\mathbf{curl}\, \boldsymbol{M}\|,$$

which indicates that

$$\|R_{\boldsymbol{A}}^n\|_{(\boldsymbol{H}(\mathbf{curl},\Omega))'} \leq \sup_{\boldsymbol{0} \neq \boldsymbol{M} \in D} \frac{(R_{\boldsymbol{A}}^n, \boldsymbol{M})}{\|\boldsymbol{M}\|_{\boldsymbol{H}(\mathbf{curl},\Omega)}} \leq C\tau \|\boldsymbol{H}_t\|_{L^\infty(t_{n-1},t_n;\boldsymbol{L}^2(\Omega))}. \tag{50}$$

With this result, we can regain the full order of τ in (30) by using (49) and triangle inequality. This completes the proof. $\qquad\square$

Remark 5.5. For the error estimate for $\boldsymbol{A}$ in the scheme (19), the truncation term $R_{\boldsymbol{A}}^n$ enters into the error equations, which further leads to the estimate (49). Hence, with the regularity (27), we only get the suboptimal convergence order in time for $\boldsymbol{A}$ with half an order lost. With a slightly stronger regularity assumption with $\boldsymbol{H}_t \in L^\infty(0,T;\boldsymbol{L}^2(\Omega))$, we improve the estimate of $R_{\boldsymbol{A}}^n$ and regain the full order of τ. But this issue does not arise during the error estimate for the scheme (A.1), we refer to Appendix A for more details.

TABLE 1. Errors and convergence rates for time discretization.

τ	$\left\|e_{\boldsymbol{u}}^N\right\|$	$\left\|\nabla e_{\boldsymbol{u}}^N\right\|$	$\left\|e_p^N\right\|$	$\left\|e_{\boldsymbol{H}}^N\right\|$
0.2	1.98e−04(−)	2.16e−03(−)	3.70e−02(−)	4.19e−03(−)
0.1	9.94e−05(0.99)	1.09e−03(0.99)	1.87e−02(0.98)	2.09e−03(1.00)
0.05	4.98e−05(1.00)	5.46e−04(1.00)	9.42e−03(0.99)	1.04e−03(1.00)
0.025	2.50e−05(1.00)	2.73e−04(1.00)	4.72e−03(1.00)	5.22e−04(1.00)

τ	$\left\|\mathbf{curl}\, e_{\boldsymbol{H}}^N\right\|$	$\left\|e_{\boldsymbol{A}}^N\right\|$	$\left\|\mathbf{curl}\, e_{\boldsymbol{A}}^N\right\|$
0.2	1.88e−02(−)	8.84e−04(−)	3.96e−03(−)
0.1	9.38e−03(1.00)	4.34e−04(1.03)	1.95e−03(1.03)
0.05	4.68e−03(1.00)	2.15e−04(1.01)	9.66e−04(1.01)
0.025	2.34e−03(1.00)	1.07e−04(1.01)	4.81e−04(1.01)

Remark 5.6. Invoking with (45)–(47) and Lemma 5.3, we derive carefully to get a more elaborate expression for the constant on the right-hand side of (48),

$$C = \exp\big(C_1\big(R_e, R_e\kappa^2, R_m\kappa\big)T\big)C_2\big(R_e, R_e^3, R_m\kappa, R_e\kappa^2\big).$$

Here we use the notation $C_i(\cdot)$ to indicate that the constant C_i depend on the "$\cdot$", $i = 1, 2$. Clearly, one can see that the constant C on the right-hand side of (48) heavily depends on the the Reynolds number, the magnetic Reynolds number and the coupling number. Therefore, the error estimates obtained will deteriorate with these physical parameters increase.

6. NUMERICAL EXPERIMENTS

In this section, we give some numerical experiments to validate the accuracy and stability of the scheme. All simulations are run using the finite element software FreeFEM [20].

Example 6.1 (Convergence rate for time discretization)**.** This example is to validate the convergence orders of the time discretization. The computational domain is taken as $\Omega = (0, 1)^3$ and the parameters are set by $R_e = R_m = \kappa = 1$. We choose the right-hand sides, initial and boundary conditions such that the considered system admits the following exact solutions,

$$\boldsymbol{u} = (z\sin(t), x\exp(-t), y\cos(t)), \; p = (x + y + z)\cos(t), \; \phi = 0,$$
$$\boldsymbol{H} = (\cos(t), \sin(t), \exp(-t)), \; \boldsymbol{A} = (\cos(t), \exp(-t), \sin(t)).$$

Since the exact solutions are linear or constant in spatial variables, the errors only come from the discretization of the time variable. We fix a tetrahedron mesh with $h = 1/4$ and the terminal time $T = 1$. The numerical results with different time steps are listed in Table 1. We observe that the expected first-order convergence is obtained for the scheme, which is consistent with the error estimates in Theorem 4.3.

Example 6.2 (Convergence rate for full discretization)**.** This example is to test the convergence rates for the fully discretization. The computational domain is taken as $\Omega = (0, 1)^3$, the physical parameters are set by $R_e = R_m = \kappa = 1$ and the terminal time is given by $T = 1$. The right-hand sides, initial and boundary conditions are chosen so that the exact solutions are given by

$$\boldsymbol{u} = (\cos(z)\sin(t), \sin(x)\exp(-t), \sin(y)\cos(t)), \; p = \sin(x + y + z)\cos(t), \; \phi = 0,$$
$$\boldsymbol{H} = (\sin(y)\cos(t), \cos(z)\sin(t), \cos(x)\exp(-t)), \; \boldsymbol{A} = (\cos(y)\cos(t), \sin(z)\exp(-t), \sin(x)\sin(t)).$$

TABLE 2. Errors and convergence rates for the fully discrete scheme.

(τ, h)	$\left\|\nabla e_{\boldsymbol{u}}^N\right\|$	$\left\|e_p^N\right\|$	$\left\|e_{\boldsymbol{H}}^N\right\|$	$\left\|\mathbf{curl}\, e_{\boldsymbol{H}}^N\right\|$
(τ_0, h_0)	1.13e−01(−)	7.33e−02(−)	8.42e−02(−)	9.82e−02(−)
$(\tau_0, h_0)/2$	5.63e−02(1.00)	1.97e−02(1.90)	4.25e−02(0.99)	4.95e−02(0.99)
$(\tau_0, h_0)/4$	2.81e−02(1.00)	7.16e−03(1.46)	2.13e−02(1.00)	2.49e−02(0.99)
$(\tau_0, h_0)/8$	1.41e−02(1.00)	3.08e−03(1.22)	1.07e−02(1.00)	1.25e−02(1.00)

(τ, h)	$\left\|e_{\boldsymbol{A}}^N\right\|$	$\left\|\mathbf{curl}\, e_{\boldsymbol{A}}^N\right\|$
(τ_0, h_0)	9.61e−02(−)	7.58e−02(−)
$(\tau_0, h_0)/2$	5.53e−02(0.80)	3.83e−02(0.99)
$(\tau_0, h_0)/4$	2.90e−02(0.93)	1.92e−02(1.00)
$(\tau_0, h_0)/8$	1.47e−02(0.98)	9.60e−03(1.00)

(τ, h)	$\left\|e_{\boldsymbol{u}}^N\right\|$
(τ_0, h_0)	1.80e−02(−)
$(\tau_0/4, h_0/2)$	4.52e−03(2.00)
$(\tau_0/16, h_0/4)$	1.13e−03(2.00)
$(\tau_0/64, h_0/8)$	2.83e−04(2.00)

The initial mesh size and time step are set by $h = 1/2$ and $\tau = 1/5$. We fist refine the time step and the mesh size at the same time such that $\tau = Ch$ to test the convergence of $\boldsymbol{H}^1$-error for $\boldsymbol{u}$, $\boldsymbol{H}(\mathbf{curl})$-errors for $\boldsymbol{H}$ and $\boldsymbol{A}$, the L^2-errors for p, $\boldsymbol{H}$ and $\boldsymbol{A}$. Next, to test the convergence of L^2-error for $\boldsymbol{u}$, we refine the time step and the mesh size simultaneously such that $\tau = Ch^2$. The corresponding results are displayed in Table 2. We can see that the discrete solutions have the asymptotic behaviors,

$$\left\|\boldsymbol{u}(T) - \boldsymbol{u}_h^N\right\| = \mathcal{O}\left(\tau + h^2\right), \quad \left\|\nabla \boldsymbol{u}(T) - \nabla \boldsymbol{u}_h^N\right\| = \mathcal{O}(\tau + h), \quad \left\|p(T) - p_h^N\right\| = \mathcal{O}(\tau + h),$$
$$\left\|\boldsymbol{H}(T) - \boldsymbol{H}_h^N\right\| = \mathcal{O}(\tau + h), \quad \left\|\boldsymbol{A}(T) - \boldsymbol{A}_h^N\right\| = \mathcal{O}(\tau + h),$$
$$\left\|\mathbf{curl}\,\boldsymbol{H}(T) - \mathbf{curl}\,\boldsymbol{H}_h^N\right\| = \mathcal{O}(\tau + h), \quad \left\|\mathbf{curl}\,\boldsymbol{A}(T) - \mathbf{curl}\,\boldsymbol{A}_h^N\right\| = \mathcal{O}(\tau + h).$$

In other words, the expected convergence rates of the proposed numerical scheme can be observed, which agrees with Theorem 4.3. The unconditional and optimal error estimates will be our further work.

Example 6.3 (Unconditional energy stability). This example is to test the unconditional energy stability of the proposed scheme. We take the domain as $\Omega = (0,1)^3$ and set the initial conditions for $\boldsymbol{u}$ and $\boldsymbol{H}$ to be

$$\boldsymbol{u}^0 = -\pi/2 \sin(\pi x) \sin(\pi y) \sin(\pi z)\boldsymbol{\Psi}, \quad \boldsymbol{H}^0 = -1/2 xyz(x-1)(y-1)(z-1)\Phi,$$
$$\boldsymbol{\Psi} = (\sin(\pi x)\cos(\pi y)\cos(\pi z), -2\cos(\pi x)\sin(\pi y)\cos(\pi z), \cos(\pi x)\cos(\pi y)\sin(\pi z)),$$
$$\Phi = (x(x-1)(2y-1)(2z-1), -2y(y-1)(2x-1)(2z-1), z(z-1)(2x-1)(2y-1)).$$

With the given data, we test the energy stability of our scheme under different physical parameters and time steps on a fixed mesh with $h = 1/16$. Denote the discrete energy at t_n by $\mathrm{E}_h^n = \left(\|\boldsymbol{u}_h^n\|^2 + \kappa\|\boldsymbol{H}_h^n\|^2\right)/2$, Figure 1 shows the time evolution of the discrete energy with the finial time $T = 5$. It can be observed that all energy curves decrease monotonically, which means that our scheme is unconditionally energy stable.

Example 6.4 (Driven cavity flow). In this example, we simulate the benchmark problem of driven cavity flow. The problem models the flow of a conducting fluid driven by the movement of the lid at the top of the
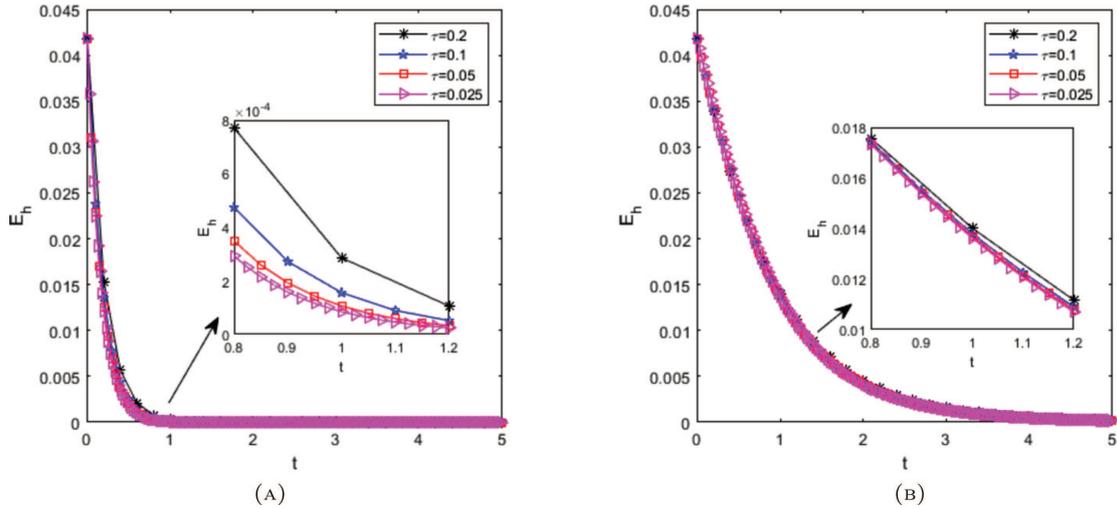
FIGURE 1. Time evolution of the energy with different time step sizes. (a) $R_e = R_m = 30$ and $\kappa = 1$. (b) $R_e = R_m = 200$ and $\kappa = 5$.

cavity under the external magnetic field. When the external magnetic field is zero, the problem becomes the classical hydrodynamic lid-driven cavity problem. For this end, we set $\Omega = (0,1)^3$ and take the initial values as $\boldsymbol{H}_0 = (-1,0,0)$ and $\boldsymbol{u}_0 = (g_1,0,0)^{\mathrm{T}}$, where $g_1 = g_1(z)$ is a continuous function and satisfies

$$g_1(x,y,1) = 1, \quad \text{and} \quad g_1(x,y,z) = 0 \quad \forall z \in [0, 1-h],$$

where h is the mesh size. Let $\boldsymbol{A}_b = (0,0,-y)$, the boundary conditions are set by

$$\boldsymbol{u} = \boldsymbol{u}_0, \ \boldsymbol{H} \times \boldsymbol{n} = \boldsymbol{H}_0 \times \boldsymbol{n}, \ \boldsymbol{A} \cdot \boldsymbol{n} = \boldsymbol{A}_b \cdot \boldsymbol{n}, \ \mathbf{curl}\,\boldsymbol{A} \times \boldsymbol{n} = \mathbf{curl}\,\boldsymbol{A}_b \times \boldsymbol{n}, \ \text{on } \Gamma.$$

To compare our results with those in [29], the physical parameters are set by $R_e = 100$, $R_m = 10$ and $\kappa = 1$. In the computation, we set the mesh size $h = 1/32$, the time step $\tau = 0.01$, and the finial time $T = 5$. In Figure 2, we display the streamlines of velocity on the three cross-sections $x = 0.5$, $y = 0.5$ and $z = 0.5$, respectively. They show clearly the vortex structure of the fluid. Note that our result on the cross-section $y = 0.5$ is in agreement well with the previous result in [29], which studied the steady CT-MHD model. Figure 3 shows the distributions of $|\boldsymbol{H}_h|$ and Figure 4 shows the magnetic vector potential $\boldsymbol{A}_h$ on the three cross-sections $x = 0.5$, $y = 0.5$ and $z = 0.5$, respectively. From these figures, we can know how the fluid influences the electromagnetic fields.

7. CONCLUSIONS

In this paper, we study a fully discrete finite element scheme for the CT-MHD model. The scheme is designed by combining an Euler semi-implicit scheme for the temporal discretization and mixed finite elements for the spatial discretization. A novel feature is that it preserves the divergence-free property exactly for the magnetic induction and current density on the discrete level. Error estimates for the velocity, magnetic field and magnetic vector potential are further established under the low regularity hypothesis for the exact solutions. Some numerical experiments are presented to verify the theoretical analysis and show the performance of the proposed scheme.

Note that we use a semi-implicit backward Euler scheme in time, which is first-order accurate in the temporal direction. Apparently, one replace it by higher-order time integrator with some subtle implicit-explicit treatments for nonlinear and coupling terms, such Crank-Nicholson scheme and second-order backward difference formula
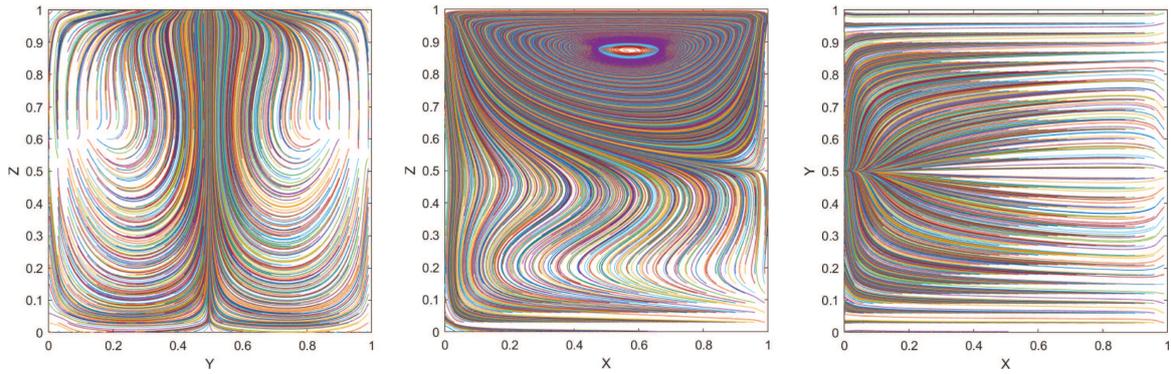
FIGURE 2. Streamlines of $\boldsymbol{u}_h$ on the cross section $x = 0.5$ (*Left*), $y = 0.5$ (*Middle*) and $z = 0.5$ (*Right*).
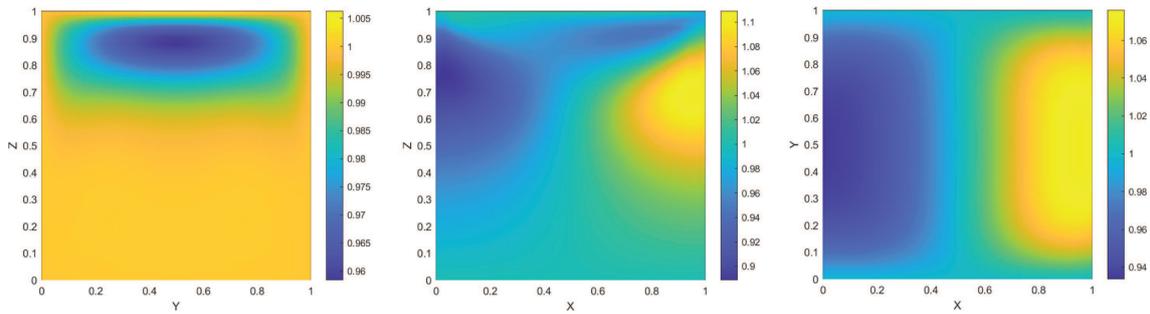

FIGURE 3. Distributions of $|\boldsymbol{H}_h|$ on the cross section $x = 0.5$ (*Left*), $y = 0.5$ (*Middle*) and $z = 0.5$ (*Right*).
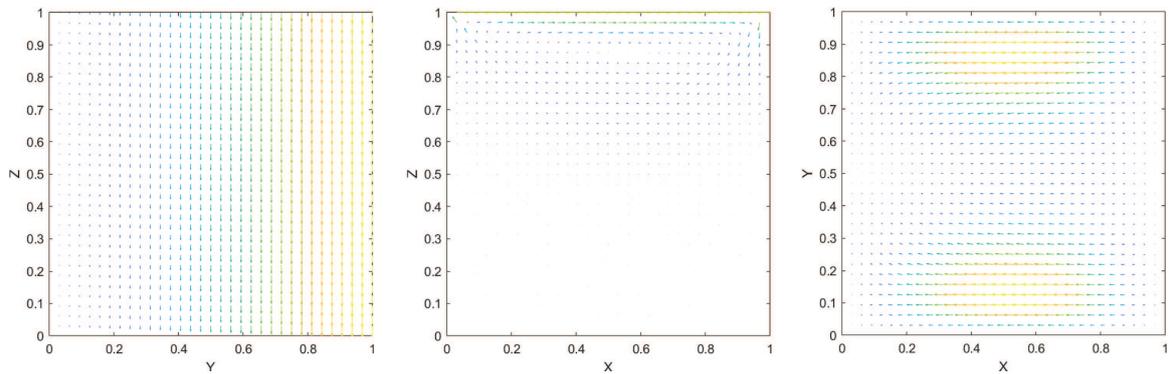

FIGURE 4. Projection of $\boldsymbol{A}_h$ on the cross section $x = 0.5$ (*Left*), $y = 0.5$ (*Middle*) and $z = 0.5$ (*Right*).

(BDF2). For instance, a semi-implicit scheme based on BDF2 is to find $(\boldsymbol{u}_h^n, p_h^n, \boldsymbol{H}_h^n, \boldsymbol{A}_h^n, \phi_h^n) \in \boldsymbol{V}_h \times Q_h \times \boldsymbol{W}_h \times$
$\boldsymbol{D}_h \times S_h$ with $n \geq 2$ such that for all $(\boldsymbol{v}_h, q_h, \boldsymbol{C}_h, \boldsymbol{M}_h, \psi_h) \in \boldsymbol{V}_h \times Q_h \times \boldsymbol{W}_h \times \boldsymbol{D}_h \times S_h$,

$$\left(\delta_t^2 \boldsymbol{u}_h^n, \boldsymbol{v}_h\right) + R_e^{-1}(\nabla \boldsymbol{u}_h^n, \nabla \boldsymbol{v}_h) + \mathcal{O}(\hat{\boldsymbol{u}}_h^n, \boldsymbol{u}_h^n, \boldsymbol{v}_h) - (p_h^n, \operatorname{div}\boldsymbol{v}_h) - \kappa(\mathbf{curl}\,\boldsymbol{H}_h^n \times \mathbf{curl}\,\boldsymbol{A}_h^n, \boldsymbol{v}_h) = 0,$$

$$(\operatorname{div}\boldsymbol{u}_h^n, q_h) = 0,$$

$$\left(\delta_t^2 \boldsymbol{H}_h^n, \boldsymbol{C}_h\right) + R_m^{-1}(\mathbf{curl}\,\boldsymbol{H}_h^n, \mathbf{curl}\,\boldsymbol{C}_h) + (\mathbf{curl}\,\boldsymbol{A}_h^n \times \boldsymbol{u}_h^n, \mathbf{curl}\,\boldsymbol{C}_h) = 0,$$

$$(\mathbf{curl}\,\boldsymbol{A}_h^n, \mathbf{curl}\,\boldsymbol{M}_h) + (\nabla \phi_h^n, \boldsymbol{M}_h) - \left(\hat{\boldsymbol{H}}_h^n, \mathbf{curl}\,\boldsymbol{M}_h\right) = 0,$$

$$(\boldsymbol{A}_h^n, \nabla \psi_h) = 0.$$

where the second-order difference operator δ_t^2 and extrapolated operator $\hat{\ }$ are defined by

$$\delta_t^2 \zeta^n := \frac{3\zeta^n - 4\zeta^{n-1} + \zeta^{n-2}}{2\tau}, \quad \hat{\zeta}^n := 2\zeta^{n-1} - \zeta^{n-2}.$$

For $n = 1$, we can use the semi-implicit Euler scheme (19) to compute $\left(\boldsymbol{u}_h^1, p_h^1, \boldsymbol{H}_h^1, \boldsymbol{A}_h^1, \phi_h^1\right)$. Provided enough temporal regularity, one can easily obtain the error estimate by a similar analysis. We believe that their analysis shall not present difficulties beyond those already encountered in this work. In the future, robust and fast solvers for this scheme will be considered.

APPENDIX A.

In this section, we give a similar fully discrete scheme to (19) and present the results of error analysis in a nutshell. Different from the treatment skills in (19), here we lag the magnetic vector potential in (19a)–(19c) to decouple it from other variables. Hence, a new fully discrete finite element scheme for problem (5) reads as follows. For any $n \geq 1$, we find $(\boldsymbol{u}_h^n, p_h^n, \boldsymbol{H}_h^n, \boldsymbol{A}_h^n, \phi_h^n) \in \boldsymbol{V}_h \times Q_h \times \boldsymbol{W}_h \times \boldsymbol{D}_h \times S_h$ such that for all $(\boldsymbol{v}_h, q_h, \boldsymbol{C}_h, \boldsymbol{M}_h, \psi_h) \in \boldsymbol{V}_h \times Q_h \times \boldsymbol{W}_h \times \boldsymbol{D}_h \times S_h$,

$$(\delta_t \boldsymbol{u}_h^n, \boldsymbol{v}_h) + R_e^{-1}(\nabla \boldsymbol{u}_h^n, \nabla \boldsymbol{v}_h) + \mathcal{O}\left(\boldsymbol{u}_h^{n-1}, \boldsymbol{u}_h^n, \boldsymbol{v}_h\right) - (p_h^n, \operatorname{div}\boldsymbol{v}_h) - \kappa\left(\mathbf{curl}\,\boldsymbol{H}_h^n \times \mathbf{curl}\,\boldsymbol{A}_h^{n-1}, \boldsymbol{v}_h\right) = 0, \quad \text{(A.1a)}$$

$$(\operatorname{div}\boldsymbol{u}_h^n, q_h) = 0, \quad \text{(A.1b)}$$

$$(\delta_t \boldsymbol{H}_h^n, \boldsymbol{C}_h) + R_m^{-1}(\mathbf{curl}\,\boldsymbol{H}_h^n, \mathbf{curl}\,\boldsymbol{C}_h) + \left(\mathbf{curl}\,\boldsymbol{A}_h^{n-1} \times \boldsymbol{u}_h^n, \mathbf{curl}\,\boldsymbol{C}_h\right) = 0, \quad \text{(A.1c)}$$

$$(\mathbf{curl}\,\boldsymbol{A}_h^n, \mathbf{curl}\,\boldsymbol{M}_h) + (\nabla \phi_h^n, \boldsymbol{M}_h) - (\boldsymbol{H}_h^n, \mathbf{curl}\,\boldsymbol{M}_h) = 0, \quad \text{(A.1d)}$$

$$(\boldsymbol{A}_h^n, \nabla \psi_h) = 0. \quad \text{(A.1e)}$$

At the initial time step, $\boldsymbol{u}_h^0 = \mathcal{P}_h \boldsymbol{u}_0$ and $\boldsymbol{H}_h^0 = \mathcal{F}_h \boldsymbol{H}_0$, where $\mathcal{P}_h$ and $\mathcal{F}_h$ are projection operators defined in Section 5. In addition, $\boldsymbol{A}_h^0$ is taken as a part of the solution $(\boldsymbol{A}_h^0, \phi_h^0)$ to the following problem,

$$\left(\mathbf{curl}\,\boldsymbol{A}_h^0, \mathbf{curl}\,\boldsymbol{M}_h\right) + \left(\nabla \phi_h^0, \boldsymbol{M}_h\right) - \left(\boldsymbol{H}_h^0, \mathbf{curl}\,\boldsymbol{M}_h\right) = 0, \quad \text{(A.2a)}$$

$$\left(\boldsymbol{A}_h^0, \nabla \psi_h\right) = 0, \quad \text{(A.2b)}$$

for all $(\boldsymbol{M}_h, \psi_h) \in \boldsymbol{D}_h \times S_h$. As we discussed in Remark 3.4, we can carry out the new scheme (A.1) by first solving the discrete problem (A.1a)–(A.1c) for $(\boldsymbol{u}, p, \boldsymbol{H})$ and then solving the discrete problem (A.1d) and (A.1e) for $(\boldsymbol{A}, \phi)$. Therefore, the cost of calculation for these two schemes (19) and (A.1) are almost same except a extra cost of the computation for $\boldsymbol{A}_h^0$ in (A.1). In fact, this is just a trick of index for (19) and (A.1). If we write the solutions to (A.1) as $\left(\hat{\boldsymbol{u}}_h^n, \hat{p}_h^n, \hat{\boldsymbol{H}}_h^n, \hat{\boldsymbol{A}}_h^n, \hat{\phi}_h^n\right)$, then there holds the following relation for $1 \leq n \leq N - 1$,

$$\left(\hat{\boldsymbol{u}}_h^n, \hat{p}_h^n, \hat{\boldsymbol{H}}_h^n\right) = (\boldsymbol{u}_h^n, p_h^n, \boldsymbol{H}_h^n), \quad \left(\hat{\boldsymbol{A}}_h^n, \hat{\phi}_h^n\right) = \left(\boldsymbol{A}_h^{n+1}, \phi_h^{n+1}\right).$$

and for $n = 0$,

$$\left(\hat{\boldsymbol{u}}_h^0, \hat{\boldsymbol{H}}_h^0\right) = \left(\boldsymbol{u}_h^0, \boldsymbol{H}_h^0\right), \quad \left(\hat{\boldsymbol{A}}_h^0, \hat{\phi}_h^0\right) = \left(\boldsymbol{A}_h^1, \phi_h^1\right).$$

Next, we state the unique solvability and stability of the scheme (A.1) is the following theorem, which mimics Theorems 4.1 and 4.2.

Theorem A.1. *For any $\tau > 0$ and $h > 0$, the scheme (A.1) is uniquely solvable at each time step. Furthermore, the discrete solution $(\boldsymbol{u}_h^n, p_h^n, \boldsymbol{H}_h^n, \boldsymbol{A}_h^n, \phi_h^n)$ satisfies*

$$\frac{\|\boldsymbol{u}_h^n\|^2 - \|\boldsymbol{u}_h^{n-1}\|^2 + \|\boldsymbol{u}_h^n - \boldsymbol{u}_h^{n-1}\|^2}{2\tau} + \kappa \frac{\|\boldsymbol{H}_h^n\|^2 - \|\boldsymbol{H}_h^{n-1}\|^2 + \|\boldsymbol{H}_h^n - \boldsymbol{H}_h^{n-1}\|^2}{2\tau}$$
$$+ R_e^{-1}\|\nabla\boldsymbol{u}_h^n\|^2 + \kappa R_m^{-1}\|\mathbf{curl}\,\boldsymbol{H}_h^n\|^2 = 0, \tag{A.3}$$
$$\|\mathbf{curl}\,\boldsymbol{A}_h^n\| \leq \|\boldsymbol{H}_h^n\|. \tag{A.4}$$

Consequently, we have the following estimates for $m = 1, 2, \cdots, N$,

$$\|\boldsymbol{u}_h^m\|^2 + \kappa\|\boldsymbol{H}_h^m\|^2 + 2\tau\sum_{n=1}^m \Big(R_e^{-1}\|\nabla\boldsymbol{u}_h^n\|^2 + \kappa R_m^{-1}\|\mathbf{curl}\,\boldsymbol{H}_h^n\|^2 \Big) \leq \|\boldsymbol{u}_h^0\|^2 + \kappa\|\boldsymbol{H}_h^0\|^2, \tag{A.5}$$

$$\kappa\|\mathbf{curl}\,\boldsymbol{A}_h^m\|^2 \leq \|\boldsymbol{u}_h^0\|^2 + \kappa\|\boldsymbol{H}_h^0\|^2. \tag{A.6}$$

For the error estimates, we assume that the exact solution of MHD system (5) uniquely exists and the unknowns have following regularity property:

$$\begin{aligned}
&\boldsymbol{u} \in L^\infty(0,T;\boldsymbol{H}^{1+s}(\Omega)),\ \boldsymbol{u}_t \in L^2(0,T;\boldsymbol{H}^{1+s}(\Omega)),\ \boldsymbol{u}_{tt} \in L^2(0,T;\boldsymbol{H}^{-1}(\Omega)),\\
&p \in L^\infty(0,T;H^s(\Omega)),\ p_t \in L^2(0,T;H^s(\Omega)),\\
&\boldsymbol{H}, \mathbf{curl}\,\boldsymbol{H}, \boldsymbol{A}, \mathbf{curl}\,\boldsymbol{A} \in L^\infty(0,T;\boldsymbol{H}^s(\Omega)),\\
&\boldsymbol{H}_t, \mathbf{curl}\,\boldsymbol{H}_t \in L^2(0,T;\boldsymbol{H}^s(\Omega)),\ \boldsymbol{H}_{tt} \in L^2\big(0,T;(\boldsymbol{H}(\mathbf{curl},\Omega))'\big),\\
&\mathbf{curl}\,\boldsymbol{A}_t \in L^2(0,T;\boldsymbol{L}^2(\Omega)),
\end{aligned} \tag{A.7}$$

where $s > \frac{1}{2}$. The error estimate for (A.1) can be deduced similarly as Lemma 5.4 and Theorem 4.3.

Theorem A.2. *Let $(\boldsymbol{u}, p, \boldsymbol{H}, \boldsymbol{A}, \phi)$ be the exact solution of (5) with the regularity (A.7) holds. Let $(\boldsymbol{u}_h^n, p_h^n, \boldsymbol{H}_h^n, \boldsymbol{A}_h^n, \phi_h^n)$ be the numerical solution of the discrete system (A.1). Then we have the following error estimate for all $m = 1, 2, \cdots, N$,*

$$\|\boldsymbol{u}^m - \boldsymbol{u}_h^m\|^2 + \kappa\|\boldsymbol{H}^m - \boldsymbol{H}_h^m\|^2 + \|\mathbf{curl}\,(\boldsymbol{A}^m - \boldsymbol{A}_h^m)\|^2$$
$$+ 2\tau\sum_{n=1}^m \Big(R_e^{-1}\|\nabla(\boldsymbol{u}^n - \boldsymbol{u}_h^n)\|^2 + \kappa R_m^{-1}\|\mathbf{curl}\,(\boldsymbol{H}^n - \boldsymbol{H}_h^n)\|^2 \Big) \leq C(h^{2\beta} + \tau^2), \tag{A.8}$$

with $\beta = \min\{s, k\}$ and C is independent of the discrete parameters τ and h.

In the proof of the error estimate for $\boldsymbol{A}$ in the scheme (A.1), the truncation term $R_{\boldsymbol{A}}^n$ vanishes in the error equations due to the treatment of $\boldsymbol{A}$ and $\boldsymbol{H}$ in (A.1d) at the same time level. As a result, we can derive the optimal convergence rate in time straightway. But it's a pity that we have introduce a slightly stronger regularity assumption with $\mathbf{curl}\,\boldsymbol{A}_t \in L^2(0,T;\boldsymbol{L}^2(\Omega))$ by comparing (27) with (A.7).

References

[1] D.N. Arnold, R.S. Falk and R. Winther, Finite element exterior calculus, homological techniques, and applications. *Acta Numer.* **15** (2006) 1–155.

[2] D. Boffi, Fortin operator and discrete compactness for edge elements. *Numer. Math.* **87** (2000) 229–246.

[3] D. Boffi, F. Brezzi and M. Fortin, Mixed Finite Element Methods and Applications. Vol. 44 of *Springer Series in Computational Mathematics*. Springer, Heidelberg (2013).

[4] J.U. Brackbill and D.C. Barnes, The effect of nonzero $\nabla \cdot \boldsymbol{B}$ on the numerical solution of the magnetohydrodynamic equations. *J. Comput. Phys.* **35** (1980) 426–430.

[5] B. Cockburn, G. Kanschat and D. Schötzau, A nonote on discontinuous Galerkin divergence-free solutions of the Navier–Stokes equations. *J. Sci. Comput.* **31** (2007) 61–73.

[6] M. Costabel and M. Dauge, Singularities of Maxwell's equations on polyhedral domains, in Analysis, Numerics and Applications of Differential and Integral Equations (Stuttgart, 1996). Vol. 379 of *Pitman Res. NONOTEs Math. Ser.* Longman, Harlow (1998) 69–76.

[7] M. Costabel and M. Dauge, Singularities of electromagnetic fields in polyhedral domains. *Arch. Ration. Mech. Anal.* **151** (2000) 221–276.

[8] W. Dai and P.R. Woodward, On the divergence-free condition and conservation laws in numerical simulations for supersonic magnetohydrodynamical flows. *Astrophys. J.* **494** (1998) 317–335.

[9] P.A. Davidson, An Introduction to Magnetohydrodynamics. *Cambridge Texts in Applied Mathematics*. Cambridge University Press, Cambridge (2001).

[10] Q. Ding, X. Long and S. Mao, Convergence analysis of Crank-Nicolson extrapolated fully discrete scheme for thermally coupled incompressible magnetohydrodynamic system. *Appl. Numer. Math.* **157** (2020) 522–543.

[11] H. Duan, S. Li, R.C.E. Tan and W. Zheng, A delta-regularization finite element method for a double cnourl problem with divergence-free constraint. *SIAM J. Numer. Anal.* **50** (2012) 3208–3230.

[12] K.J. Galvin, A. Linke, L.G. Rebholz and N.E. Wilson, Stabilizing poor mass conservation in incompressible flow problems with large irrotational forcing and application to thermal convection. *Comput. Methods Appl. Mech. Eng.* **237/240** (2012) 166–176.

[13] H. Gao and W. Qiu, A semi-implicit energy conserving finite element method for the dynamical incompressible magnetohydrodynamics equations. *Comput. Methods Appl. Mech. Eng.* **346** (2019) 982–1001.

[14] J.-F. Gerbeau, C. Le Bris and T. Lelièvre, Mathematical Methods for the Magnetohydrodynamics of Liquid Metals. *Numerical Mathematics and Scientific Computation*. Oxford University Press, Oxford (2006).

[15] V. Girault and P.-A. Raviart, Finite Element Methods for Navier–Stokes Equations. Vol. 5 of *Springer Series in Computational Mathematics*. Springer-Verlag, Berlin (1986).

[16] C. Greif, D. Li, D. Schötzau and X. Wei, A mixed finite element method with exactly divergence-free velocities for incompressible magnetohydrodynamics. *Comput. Methods Appl. Mech. Eng.* **199** (2010) 2840–2855.

[17] M.D. Gunzburger, A.J. Meir and J.S. Peterson, On the existence, uniqueness, and finite element approximation of solutions of the equations of stationary, incompressible magnetohydrodynamics. *Math. Comput.* **56** (1991) 523–563.

[18] J. He, K. Hu and J. Xu, Generalized Gaffney inequality and discrete compactness for discrete differential forms. *Numer. Math.* **143** (2019) 781–795.

[19] Y. He, Unconditional convergence of the Euler semi-implicit scheme for the three-dimensional incompressible MHD equations. *IMA J. Numer. Anal.* **35** (2015) 767–801.

[20] F. Hecht, New development in FreeFem++. *J. Numer. Math.* **20** (2012) 251–265.

[21] R. Hiptmair, Finite elements in computational electromagnetism. *Acta Numer.* **11** (2002) 237–339.

[22] R. Hiptmair, L. Li, S. Mao and W. Zheng, A fully divergence-free finite element method for magnetohydrodynamic equations. *Math. Models Methods Appl. Sci.* **28** (2018) 659–695.

[23] K. Hu, Y. Ma and J. Xu, Stable finite element methods preserving $\nabla \cdot B = 0$ exactly for MHD models. *Numer. Math.* **135** (2017) 371–396.

[24] V. John, Finite Element Methods for Incompressible Flow Problems. Vol. 51 of *Springer Series in Computational Mathematics*. Springer, Cham (2016).

[25] V. John, A. Linke, C. Merdon, M. Neilan and L.G. Rebholz, On the divergence constraint in mixed finite element methods for incompressible flows. *SIAM Rev.* **59** (2017) 492–544.

[26] L. Li, *Finite element methods and fast solvers for incompressible magetohydrodynamic systems*. Ph.D. thesis, AMSS, Chinese Academy of Sciences (2018).

[27] L. Li, M. Ni and W. Zheng, A charge-conservative finite element method for inductionless MHD equations. Part I: convergence. *SIAM J. Sci. Comput.* **41** (2019) B796–B815.

[28] L. Li, M. Ni and W. Zheng, A charge-conservative finite element method for inductionless MHD equations. Part II: a robust solver. *SIAM J. Sci. Comput.* **41** (2019) B816–B842.

[29] L. Li, D. Zhang and W. Zheng, A constrained transport divergence-free finite element method for incompressible MHD equations. *J. Comput. Phys.* **428** (2021) 109980.

[30] P. Monk, Finite Element Methods for Maxwell's Equations. Numerical Mathematics and Scientific Computation. Oxford University Press, New York (2003).

[31] M.-J. Ni and J.-F. Li, A consistent and conservative scheme for incompressible MHD flows at a low magnetic Reynolds number. Part III: on a staggered mesh. *J. Comput. Phys.* **231** (2012) 281–298.

[32] M.-J. Ni, R. Munipalli, P. Huang, N.B. Morley and M.A. Abdou, A current density conservative scheme for incompressible MHD flows at a low magnetic Reynolds number. II. On an arbitrary collocated mesh. *J. Comput. Phys.* **227** (2007) 205–228.

[33] M.-J. Ni, R. Munipalli, N.B. Morley, P. Huang and M.A. Abdou, A current density conservative scheme for incompressible MHD flows at a low magnetic Reynolds number. I. On a rectangular collocated grid system. *J. Comput. Phys.* **227** (2007) 174–204.

[34] A. Prohl, Convergent finite element discretizations of the nonstationary incompressible magnetohydrodynamics system. *M2AN Math. Model. Numer. Anal.* **42** (2008) 1065–1087.

[35] W. Qiu and K. Shi, Analysis of a semi-implicit structure-preserving finite element method for the nonstationary incompressible magnetohydrodynamics equations. *Comput. Math. Appl.* **80** (2020) 2150–2161.

[36] D. Schötzau, Mixed finite element methods for stationary incompressible magneto-hydrodynamics. *Numer. Math.* **96** (2004) 771–800.

[37] G. Tóth, The $\nabla \cdot \boldsymbol{B} = 0$ constraint in shock-capturing magnetohydrodynamics codes. *J. Comput. Phys.* **161** (2000) 605–652.

[38] X. Zhang and Q. Ding, Coupled iterative analysis for stationary inductionless magnetohydrodynamic system based on charge-conservative finite element method. *J. Sci. Comput.* **88** (2021) 1–32.

[39] X. Zhang and Q. Ding, A decoupled, unconditionally energy stable and charge-conservative finite element method for inductionless magnetohydrodynamic equations. *Comput. Math. Appl.* **127** (2022) 80–96.

[40] X. Zhang and X. Wang, A fully divergence-free finite element scheme for stationary inductionless magnetohydrodynamic equations. *J. Sci. Comput.* **90** (2022) 70.

[41] G. Zhang, Y. He and D. Yang, Analysis of coupling iterations based on the finite element method for stationary magnetohydrodynamics on a general domain. *Comput. Math. Appl.* **68** (2014) 770–788.

[42] G. Zhang, J. Yang and C. Bi, Second order unconditionally convergent and energy stable linearized scheme for MHD equations. *Adv. Comput. Math.* **44** (2018) 505–540.

[43] J. Zhao, Analysis of finite element approximation for time-dependent Maxwell problems. *Math. Comput.* **73** (2004) 1089–1105.